DEPARTMENT OF ECONOMICS WORKING PAPER SERIES

Unpacking trend inflation: Evidence from a factor correlated unobserved components model of sticky and flexible prices

Mengheng Li
Ivan Mendieta-Muñoz

Working Paper No: 2025-04

July 2025

University of Utah
Department of Economics
260 S. Central Campus Dr., GC. 4100
Tel: (801) 581-7481
Fax: (801) 585-5649
http://www.econ.utah.edu

Unpacking trend inflation: Evidence from a factor correlated unobserved components model of sticky and flexible prices*

Mengheng Li†

Ivan Mendieta-Muñoz‡

July 4, 2025

We propose a factor correlated unobserved components (FCUC) model to analyze the sticky and flexible components of U.S. inflation. The proposed FCUC framework estimates trend inflation and component cycles in a flexible stochastic environment with time-varying volatility, factor loadings, and cross-frequency (trend-cycle) correlations, thus capturing how structural heterogeneity in price adjustment shapes the evolution of aggregate trend inflation over time. Using Bayesian estimation methods, we show that the FCUC model substantially reduces the uncertainty surrounding estimates of trend inflation and improves both point and density forecast accuracy. Our findings reveal that, particularly following the Global Financial Crisis and more markedly since the COVID-19 recession, transitory price shocks originating from flexible inflation have become a major driver of trend inflation, whereas sticky inflation explains only part of the variation. These results indicate that temporary price movements can have persistent effects, highlighting important policy implications regarding the cyclical dynamics of disaggregated inflation components amid evolving macroeconomic conditions.

Keywords: trend inflation; sticky inflation; flexible inflation; stochastic volatility; dynamic factor model.

JEL Classification: C32; C53; E37.

*We are deeply grateful to Bruce Preston, Christopher Gibbs, James Morley, Mariano Kulish, Pär Österholm, and participants at the 2025 Sydney Macro Reading Group Workshop for their valuable comments and feedback.

†Senior Lecturer (Assistant Professor). University of Technology Sydney (UTS) Business School and Centre for Applied Macroeconomic Analysis (CAMA). Email: mengheng.li@uts.edu.au.

‡Associate Professor. Department of Economics, University of Utah. Email: ivan.mendietamunoz@utah.edu.

1 Introduction

The recent surge in U.S. inflation following the COVID-19 pandemic reflects a mix of persistent and transitory shocks, which are exacerbated by heightened macroeconomic uncertainty and potential changes in long-run inflation expectations. Although some Fed's communications and briefs (Daly, 2022; Jordá et al., 2022; Lansing, 2022) argue that persistent shocks have increasingly affected inflation since 2021, the uncertainty associated with the strength of the post COVID-19 economic recovery and various global supply disruptions (*e.g.*, the ongoing global energy crisis and the Russo-Ukrainian War) complicates economic policies that rely upon the estimation and measurement of trend inflation because these phenomena imply that volatile transitory shocks can effect the long-run dynamics of both inflation and inflation expectations.

In this regard, separating permanent and transitory movements in inflation remains a core task for monetary authorities, especially since major disruptions such as the Global Financial Crisis (GFC) and the pandemic tend to substantially increase economic uncertainty (Bernanke and Blanchard, 2024). The unobserved components model with stochastic volatility (UCSV model) of Stock and Watson (2007) represents a notable framework that distinguishes between permanent and transitory fluctuations of inflation dynamics since these shocks directly connect with the concepts of trend inflation and inflation cycle, respectively. Although periods of heightened uncertainty introduce complex shocks dynamics that weaken the identification of inflation signals and complicate policy calibration (Lenza and Primiceri, 2022; Comerford, 2024; Dao et al., 2024), the UCSV framework addresses this complication by allowing for stochastic (or time-varying) permanent and transitory volatilities and enabling a data-driven variance decomposition of trend inflation. This feature has made UCSV models a dominant tool for inflation forecasting and has led to numerous extensions—see, *e.g.*, Chan (2017), Chan et al. (2018), Hwu and Kim (2019), Li and Koopman (2021) and Eo et al. (2023).

Nevertheless, aggregate inflation can offer limited policy guidance during periods of economic uncertainty, as it obscures category-specific price movements that can reveal important insights about the transmission of permanent and transitory shocks in the economy (see, *e.g.*, the discussions provided by Imbs et al., 2011, Foerster et al., 2022 and Rubbo, 2024). This observation has spawned contributions that aim to improve the estimates of trend inflation by using disaggregated prices. For example, Stock and Watson (2016) introduced a factor UCSV model using seventeen personal consumption expenditure (PCE) inflation

components, while Eo et al. (2023) showed that a simpler bivariate UCSV model for manufacturing and service inflation tends to outperform the factor UCSV model—mainly because of reduced model uncertainty, and Chan et al. (2018) further improved the estimation of trend inflation by anchoring a UCSV model to survey-based long-run inflation expectations.

Following these developments, we propose a flexible factor correlated unobserved components (FCUC) model to capture key features of the U.S. headline consumer price index (CPI) inflation. Specifically, we focus on the simultaneous trend-cycle decomposition of its sticky (infrequently changing) and flexible (frequently changing) components, an important structural distinction emphasized by Bils and Klenow (2004), Bryan and Meyer (2010), and recently by Stock and Watson (2020). Since sticky prices tend to incorporate more forward-looking information and flexible prices tend to be more sensitive to contemporaneous economic conditions and slack (*e.g.*, the unemployment and output gaps), modeling their joint trend-cycle dynamics can track the relevant changes in aggregate inflation persistence more accurately. Hence, our FCUC framework exploits this structural heterogeneity to better identify the sources of inflation variation with policy-relevant inference.[1]

We make three contributions. Firstly, recognizing that the trend inflation and the inflation cycle capture low- and high-frequency price dynamics, respectively, our main innovation is to allow for time-varying cross-frequency correlations, that is, time-varying correlations between trends and cycles of the disaggregated inflation time series. This contrasts with Stock and Watson (2016) and Eo et al. (2023), who modeled only within-frequency correlation, that is, correlation within trends or cycles, either via a factor structure or a non-diagonal innovation covariance matrix. While cross-frequency correlation is a well established feature of the literature on output dynamics, linked to mechanisms such as the time-to-build effect (Morley et al., 2003; Grant and Chan, 2017; Li and Mendieta-Muñoz, 2022) and output hysteresis (Li and Mendieta-Muñoz, 2024; Furlanetto et al., 2025), it has been rarely applied to the modeling of inflation dynamics in the context of UCSV models, with the exception of Hwu and Kim (2019). This omission likely stems from the reduced-form representation of aggregate inflation that limits

[1]For example, when inflation is primarily driven by flexible components, such as motor fuel or utility prices, inflationary pressures are more likely to be transitory, implying limited need for immediate policy intervention. Indeed, Lansing (2022) calls such components "benign" shocks, as their effects tend to dissipate quickly. By contrast, when sticky components, such as rental housing or education, contribute to inflation, the risk of a permanent rise in inflation increases, which warrants a stronger policy response to prevent an entrenched trend inflation and the potential de-anchoring of long-run inflation expectations.

the identification of such correlations (Trenkler and Weber, 2016; Li and Mendieta-Muñoz, 2022). In this sense, by considering the joint estimation of sticky and flexible inflation, our FCUC model: (i) contains sufficient moment conditions for point identification; (ii) provides an analytic framework that quantifies trend-cycle interactions in inflation components; and (iii) advances the understanding of how short-run shocks in the sticky and flexible inflation cycles may influence long-run inflation dynamics in the trend inflation.

Secondly, the FCUC model jointly estimates trends and cycles of sticky and flexible inflation with relevant time-varying dynamics, namely, stochastic loadings and volatility. Complementing existing multivariate UCSV and factor models, such as Stock and Watson (2016) and Hasenzagl et al. (2022), our framework captures the co-movements and differential dynamics of disaggregated inflation components while maintaining scalability. This allows for an improved model-consistent measure of aggregate trend inflation that follows closely the structural heterogeneity of price stickiness. The inclusion of stochastic loadings and volatility in both trends and cycles further allows for a variance decomposition of the contributions of flexible and sticky cycles to trend inflation that considers both volatility and correlation effects, thus offering a refined perspective on cyclically sensitive inflation beyond that of Bryan and Meyer (2010) and Stock and Watson (2020).

Thirdly, it is not uncommon that cross-frequency correlations tend to be overestimated in unobserved components models, leading to excess trend volatility due to a small-sample bias (Trenkler and Weber, 2016; Grant and Chan, 2017; Li and Mendieta-Muñoz, 2024). To mitigate the latter, we augment the FCUC model with the long-run inflation expectation time series developed by the Federal Reserve Bank of Cleveland (2022). Similar to Hasenzagl et al. (2022), inflation expectations are treated endogenously in a time-varying fashion to control for the persistence and volatility of trend inflation. Furthermore, the long-run inflation expectation time series is a market-based measure obtained from the term structure model of Haubrich et al. (2012) and estimated in a data-rich environment. This measure of inflation expectations is derived under a set of no-arbitrage conditions and anchors trend inflation by integrating information of Treasury Inflation-Protected Securities yields, inflation swaps and swaptions, inflation-indexed bonds, Blue Chip CPI forecasts, and surveys of consumers and professional forecasters. Therefore, it is a risk adjusted measure that is robust to liquidity and behavioral

biases that are known to affect survey-based expectations (Chan et al., 2018; Hasenzagl et al., 2022).

We find two main empirical results. First, after the GFC and especially since the COVID-19 recession, transitory shocks associated with flexible inflation have played an increasingly dominant role in driving trend inflation, with their contribution rising from approximately 20% to nearly 90%. This shift is caused by a strong increase in the cross-frequency correlation between the flexible inflation cycle and trend inflation, which indicates that temporary price changes can have persistent inflationary effects and that such effects have increased importantly in recent times. By contrast, the influence of the sticky inflation's cycle has declined steadily since the Great Moderation, which is consistent with the view of better-anchored long-run inflation expectations and a decreased effect of supply-driven shocks on trend inflation.

These findings suggest that flexible inflation, although typically viewed as transitory and sensitive to economic slack (Stock and Watson, 2020; Ball et al., 2022; Dao et al., 2024), can have long-run spillovers (Lansing, 2022; Bernanke and Blanchard, 2024), which contrasts with the purely price-taking behavior of the flexible sector as modeled by Aoki (2001) and Nakamura and Steinsson (2010) and, thus, warrants closer attention of monetary policy decisions (Alvarez and Lippi, 2020; Carvalho et al., 2024). On the other hand, the sticky inflation cycle has increasingly reflected transitory volatility with limited persistence on trend inflation dynamics, which supports the view that supply shocks require a more muted policy response (Hofmann et al., 2024; Shapiro, 2024).

Second, long-run inflation expectations do not represent unbiased estimates of sticky trend inflation and, therefore, the two should not be equated. Indeed, our results show that the relationship between the sticky's inflation trend and long-run inflation expectations is characterized by significant time variation. However, the information contained in long-run inflation expectations helps to reduce the estimation uncertainty of the FCUC model, correct the scale of cross-frequency correlations, and enhance the forecast accuracy of inflation models.

The remainder of the paper is structured as follows. Section 2 presents the FCUC model and outlines the Bayesian estimation procedure. Section 3 highlights how the model captures key dynamic features of the U.S. inflation *vis-à-vis* other existing approaches. Section 4 reports the empirical results and evaluates the out-of-sample forecasting performance of the model relative

to other relevant frameworks. Finally, section 5 concludes the article.

2 Model and estimation

This section is composed of three parts. First, we summarize the decomposition of inflation into its sticky and flexible components used to construct the FCUC model. Second, we introduce the specification and main details of the proposed FCUC model. Third, we briefly discuss our Bayesian estimation procedure with details presented in the online appendix.

2.1 Sticky and flexible inflation

Bils and Klenow (2004) and Bryan and Meyer (2010) analyzed items in the CPI basket that have a low and high frequency of price changes and termed their annualized price change *sticky* and *flexible* inflation, respectively. The disaggregated CPI inflation time series compiled by Bryan and Meyer (2010) allows for the following decomposition:

$$\pi_t = \omega_S \pi_t^S + \omega_F \pi_t^F, \tag{1}$$

where π_t denotes the aggregate headline CPI inflation; while π_t^S and π_t^F denote the sticky and flexible inflation components, respectively. The component weights $\omega_S = 0.701$ and $\omega_F = 0.299$ are fixed as the categories remain the same during the sample period.

2.2 A factor correlated unobserved components model

The proposed FCUC model is a factor model of sticky inflation π_t^S, flexible inflation π_t^F, and a measure of long-run inflation expectations π_t^E. Our model features stochastic loadings, stochastic volatility components, and stochastic cross-frequency correlations. For $t = 1, ..., T$, we have

$$\pi_t^S = \tau_t^C + \eta_t^S, \tag{2}$$

$$\pi_t^F = \lambda_t \tau_t^C + \eta_t^F, \tag{3}$$

$$\pi_t^E = \alpha_t + \beta_t \tau_t^C + \sigma_E(\epsilon_t^E + \phi \epsilon_{t-1}^E), \tag{4}$$

where η^S and η_t^F are the sticky and flexible inflation cycle, respectively; while σ_E and ϕ are the standard deviation and moving average (MA) coefficient, respectively, of the transitory inflation expectation error ϵ_t^E. Additionally, τ_t^C is a common trend inflation factor that is loaded onto by π_t^S and π_t^F with loadings 1 and λ_t, respectively, as well as onto π_t^E with loading β_t.

The main innovation of the FCUC model above concerns the dynamics of τ_t^C. The latter is specified as follows:

$$\tau_t^C = \tau_{t-1}^C + \gamma_t \eta_t^S + \delta_t \eta_t^F + \eta_t^C, \tag{5}$$

where η_t^C is a common trend innovation and assumed to be Gaussian and independent of other components. Importantly, the inclusion of γ_t and δ_t connects the common trend inflation with the sticky and flexible inflation cycles in a time-varying manner. Although η_t^S and η_t^F appear on the right-hand side of (5), this does not mean that the cycles affect the trend, but simply that there are cross-frequency correlations. This specification facilitates our efficient Bayesian estimation procedure, which we discuss in sections 2.3 and 3.2.

Furthermore, we consider stochastic volatility for the trend and cycle innovations. Specifically,

$$\eta_t^m = \exp\left(\frac{h_t^m}{2}\right)\epsilon_t^m, \quad m \in \{S, F, C\}. \tag{6}$$

The log-volatilities h_t^m specified in the equation above, the intercept of inflation expectations α_t in equation (4), the loadings λ_t and β_t in equations (3) and (4), and the regression coefficients γ_t and δ_t in equation (5) are modeled as independent random walks:

$$f_t = f_{t-1} + \sigma_f \epsilon_t^f, \quad f \in \{h^S, h^F, h^C, \alpha, \beta, \lambda, \gamma, \delta\}.$$

These latent dynamics capture low-frequency temporal movements that shift the FCUC system.

Lastly, ϵ_t^g, $g \in \{S, F, C, h^S, h^F, h^C, E, \alpha, \beta, \lambda, \gamma, \delta\}$, are independent standard Gaussian errors.

2.3 Bayesian estimation

We implement a Bayesian estimation procedure for the proposed FCUC model, so the inference of trend inflation simultaneously integrates both filtering and parameter uncertainty. Specifically, we use a Markov chain Monte Carlo (MCMC) sampling algorithm that approximates the posterior distribution of latent states and model parameters using the loose

prior described below.

The FCUC model's parameters include all the innovation variances and the MA coefficient. For the former, we assign independent gamma priors:

$$\sigma_g^2 \sim \Gamma(0.5, 0.5), \quad g \in \{h^S, h^F, h^C, \alpha, \beta, \lambda, \gamma, \delta, E\}.$$

Unlike the usual inverse-gamma prior, the gamma distribution does not exclude zero variance *a priori* (Bitto and Frühwirth-Schnatter, 2019), and thus nests constant trend and volatility models as special cases. The prior has 50% and 90% probability masses within $[0, 0.455)$ and $[0, 2.706)$, respectively, implying an uninformative large tail. In the online appendix we show that these posteriors are inverse Gaussian distributions, from which we can easily sample.

For the MA coefficient, we follow Chan et al. (2018) and use a truncated normal prior within $(-1, 1)$ that ensures invertibility, denoted by $TN_{(-1,1)}(.)$, but with a larger prior variance:

$$\phi \sim TN_{(-1,1)}(0, 0.25).$$

All latent states are augmented with an uninformative zero-initialization period:

$$f_0 \sim N(0, 10^6), \quad f \in \{h^S, h^F, h^C, \alpha, \beta, \lambda, \gamma, \delta\}.$$

The structure of the prior described above allows the data to decide the temporal evolution of the latent states, thus minimizing the influence of the prior distributions. The posterior computation involves the fast precision sampler of Chan and Jeliazkov (2009) and the Gaussian mixture stochastic volatility sampler of Kim et al. (1998). Full details of the MCMC algorithm are provided in the online appendix.

3 Key stylized facts of U.S. inflation: sticky and flexible components

In this section we discuss, first, how the proposed FCUC model summarized by equations (2) through (5) captures relevant stylized facts of the U.S. inflation and, second, how the FCUC model offers further flexibility and insights to better understand inflation dynamics.

Section 3.1 presents a discussion on the dynamics of sticky, flexible and aggregate inflation;

section 3.2 focuses on the role of cross-frequency stochastic correlation; and section 3.3 explains the importance of long-run inflation expectations that anchor trend inflation.

3.1 Are sticky, flexible, and aggregate inflation similar?

The seminal UCSV model of Stock and Watson (2007) has been widely known as an accurate representation of the dynamics of the U.S. inflation. It is defined by:

$$\begin{aligned} \pi_t &= \tau_t + \eta_t, \quad \eta_t = \exp\left(\frac{h_t}{2}\right)\epsilon_t \\ \tau_t &= \tau_{t-1} + \eta_t^\tau, \quad \eta_t^\tau = \exp\left(\frac{h_t^\tau}{2}\right)\epsilon_t^\tau \\ f_t &= f_{t-1} + \sigma_f \epsilon_t^f, \quad f \in \{h, h^\tau\}, \end{aligned} \tag{7}$$

where τ_t and η_t represent the trend and cycle, respectively. ϵ_t, ϵ_t^τ, ϵ_t^h, and $\epsilon_t^{h^\tau}$ are independent standard Gaussian terms.

Shephard (2015) and Li and Koopman (2021) showed that the UCSV model implies an MA forecasting function that dynamically discounts past observations, depending on the permanent (or trend) volatility $\exp(h_t^\tau/2)$ and the transitory (or cycle) volatility $\exp(h_t/2)$. This feature allows the model to attribute inflation swings during the 1970s-80s oil crises and the 2007-9 GFC to permanent and transitory changes, respectively, while tracking the Great Moderation amid the Volcker-Greenspan-Bernanke regimes. In this sense, as documented by Shephard (2015), Lansing (2022) and Jørgensen and Lansing (2024), the UCSV model allows for a dynamic signal-to-noise ratio (SNR) that captures the time-varying persistence of trend inflation.

Given the relevance of the UCSV model, as a first exercise we fit this model to π_t^S and π_t^F individually, with the respective superscripts added to τ_t and ϵ_t and their volatilities. The weighted average of the estimated sticky and flexible trends (and cycles) corresponds to the trend (and cycle) for the aggregate inflation. The estimation results are shown in figure 1.

As shown in the bottom panel, the weighted average of sticky and flexible inflation trends obtained from two separate UCSV models does not fully correspond to the trend inflation obtained from fitting the UCSV model to the aggregate inflation. Since trend inflation is unobserved, it is not possible to decide *a priori* which of the two provides superior estimates. Moreover, the error bands of $\omega_S\tau_t^S + \omega_F\tau_t^F$ are wider than that of τ_t^S, especially during the

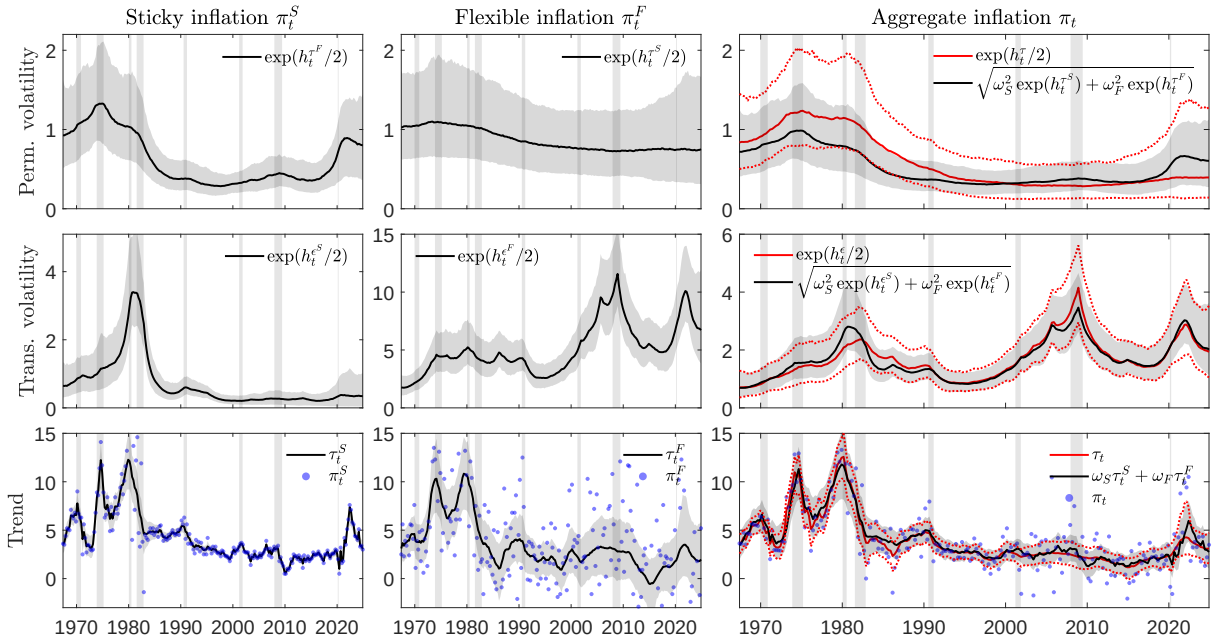

Figure 1: Permanent and transitory volatilities and trend inflation rates obtained from the UCSV model. Top to bottom: estimated permanent volatility, transitory volatility, and trend inflation. Left to right: estimation results for sticky inflation, flexible inflation, and aggregate inflation. Rightmost: red indicates aggregate inflation; whereas black shows volatilities and trend implied by the sticky-flexible inflation decomposition in (1), assuming independent components. Solid lines show the posterior medians. Shaded areas and dotted lines show the $(0.05, 0.95)$ posterior quantiles. Bottom figures were cropped for readability, with some extreme inflation values (blue dots) outside the range.

COVID-19 pandemic. This suggests that the UCSV model attributes permanent and transitory movements to the dynamics of inflation components in a different way, leading to heightened estimation uncertainty. The large transitory volatility of π_t^F during the GFC and the pandemic reduces the SNR, and thus yields a smooth τ_t^F with a large posterior variance that feeds into $\omega_S \tau_t^S + \omega_F \tau_t^F$.

These results also highlight that a separate treatment of sticky and flexible inflation overlooks the common dynamics and correlation components. Bils and Klenow (2004) and Bryan and Meyer (2010) show that some of the CPI categories have items that correspond to both sticky and flexible inflation, including some food and motor vehicle items. This means that the joint modeling of inflation trends in the FCUC model, summarized by equation (5), can better capture aggregate trend inflation dynamics when using disaggregated components of inflation (Stock and Watson, 2016). Clearly, the FCUC model implies the following aggregate trend inflation:

$$\tau_t = (\omega_S + \omega_F \lambda_t) \tau_t^C. \tag{8}$$

Let σ_t^τ denote the conditional time-varying volatility of the FCUC trend inflation derived above. Using equations (5) and (8), we have

$$\begin{aligned} \sigma_t^\tau &= |\omega_S + \omega_F \lambda_t| \sigma_t^{\tau^C}, \\ \sigma_t^{\tau^C} &= \left(\gamma_t^2 \exp(h_t^S) + \delta_t^2 \exp(h_t^F) + \exp(h_t^C)\right)^{\frac{1}{2}}, \end{aligned} \tag{9}$$

where $\sigma_t^{\tau^C}$ is the innovation volatility of τ_t^C, or common permanent volatility.

Equation (9) shows that the FCUC model allows the permanent volatility to interact with both sticky and flexible transitory volatilities in a time-varying way. Therefore, compared with the individual estimation of UCSV models, the FCUC model offers greater flexibility to track down the sources of aggregate inflation variation.

3.2 Is time-varying cross-frequency correlation present?

Standard UCSV models assume uncorrelated trends and cycles, so that permanent and transitory shocks affect the system dynamics separately. There are two types of correlations that are relevant in the context of multivariate UCSV models: (i) within-frequency correlation; and (ii) cross-frequency correlation.

Within-frequency correlation captures either the correlation between trends or the correlation between cycles, since trends and cycles capture the low- and high-frequency dynamics of the time series, respectively. Given that a trend-cycle decomposition is applied to each component of inflation, it is reasonable to assume within-frequency correlation due to overlapping item categories and the potential time variation over the business cycle. Recently, Eo et al. (2023) considered a bivariate UCSV (BUCSV) model for the inflation of manufacturing goods (MI) and services (SI) along these lines. This model considers an UCSV model, as in (7), for both MI and SI, as well as stochastic correlations between the trends and between the cycles. In doing so, it is possible to attribute aggregate trend inflation variations to those of MI and SI.

We fit the BUCSV model to sticky and flexible inflation, with the estimates of within-frequency correlations shown in figure 2. Across the whole sample period, we observe a near-perfect correlation between the trends of sticky and flexible inflation, similar to the findings in Eo et al. (2023), but no within-frequency correlation for the cycles. Hence, these BUCSV results indicate that the co-movement between sticky and flexible inflation is dominated by common temporal

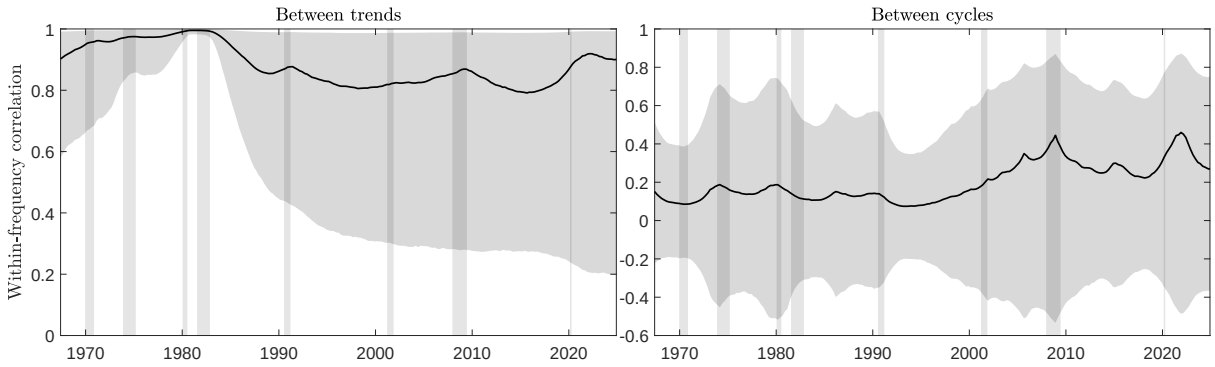

Figure 2: Within-frequency stochastic correlations obtained from the BUCSV model. We estimated the BUCSV model of Eo et al. (2023) for the sticky and flexible inflation rates. We report the stochastic correlation coefficients between trends and between cycles of sticky and flexible inflation. Lines and shaded areas indicate the posterior medians and $(0.05, 0.95)$ posterior quantiles, respectively.

patterns in the low-frequency dynamics. Indirectly, the bottom left and middle panels of figure 1 also corroborate this result.

There are two main implications derived from these findings. Firstly, the precisely estimated trend for sticky inflation, as shown in the bottom left panel of figure 1, can be incorporated into any model that aims at estimating aggregate trend inflation, especially after the 1970s-80s oil crises. We believe that this represents an advantage of the proposed sticky-flexible disaggregation over the MI-SI disaggregation, where both trends are estimated with large uncertainty compared to aggregate inflation (Eo et al., 2023). Indeed, as discussed by Bils and Klenow (2004) and more recently by Coulombe et al. (2024), sticky inflation contains highly relevant forward-looking information that is closely related to the determination of aggregate trend inflation.

Secondly, it is necessary to consider a factor model in order to model sticky and flexible inflation trends. Specifically, the near-unity correlation coefficient between trends of sticky and flexible inflation obtained from the BUCSV model suggests a single source of error. We explicitly incorporate this idea via the common factor τ_t^C, as in (2) and (3), into the proposed FCUC model. Furthermore, the stochastic loading λ_t provides additional flexibility: given λ_t, sticky and flexible trends are perfectly correlated, but otherwise their correlation is less than one. It can be shown that the conditional within-frequency correlation trends is

$$\text{Corr}_{t-1}(\tau_t^C, \lambda_t \tau_t^C) = \left[1 + \sigma_\lambda^2 \left(1 + \exp\left(-\frac{h_{t-1}^C}{2} - \frac{\sigma_{h^C}^2}{4}\right)\left(\frac{\pi_{t-1}^C}{\lambda_{t-1}}\right)^2\right)\right]^{-\frac{1}{2}} \in (0,1),$$

which is positively related to λ_{t-1}. Therefore, λ_t controls the temporal strength of the correlation between sub-component trends in the FCUC model.

As also mentioned in section 2.2, we believe that our main novelty is the introduction of cross-frequency stochastic correlation, via regression coefficients γ_t and δ_t in equation (5), which has been largely ignored in the literature on inflation modeling. Some notable exceptions are Hwu and Kim (2019), Ball et al. (2022), and Dao et al. (2024). Hwu and Kim (2019) considered trend-cycle correlation in aggregate inflation, finding that the inclusion of cross-frequency correlation improves the UCSV model's inflation forecasting performance. Ball et al. (2022) and Dao et al. (2024) found that the global inflation surge following the pandemic is accompanied by headline shocks, or transitory shocks to the deviation of headline inflation to core inflation, having strong direct and pass-through effects on core inflation. This mechanism, if present, poses challenges to the estimation of trend inflation since it requires to explicitly model how permanent and transitory shocks propagate (Bernanke and Blanchard, 2024) and undermines the optimality of monetary policy that only targets persistent price changes (Aoki, 2001; Nakamura and Steinsson, 2010; Eusepi et al., 2011).

In our FCUC model, trends are driven by the common factor τ_t^C, so we can easily compute the implied cross-frequency correlations using (5) and (9). Let ρ_t^{CS} (ρ_t^{CF}) denote the correlation between sticky (flexible) cycle innovation and trend factor innovation. We have

$$\begin{aligned} \rho_t^{CS} &= \frac{1}{\sigma_t^{\pi^C}} \gamma_t \exp\left(\frac{h_t^S}{2}\right), \\ \rho_t^{CF} &= \frac{1}{\sigma_t^{\pi^C}} \delta_t \exp\left(\frac{h_t^F}{2}\right). \end{aligned} \tag{10}$$

Hence, the proposed FCUC model also represents an extension of the correlated unobserved components (CUC) model that allows for non-zero correlation between trend and cycle innovations. The majority of CUC models focus on studying output potential and gap, and aim to explain the lasting productivity slowdown.[2] However, given the empirical and policy importance of nominal and headline shocks, as in Nakamura and Steinsson (2010), Ball et al. (2022) and Dao et al. (2024), it is clear that cross-frequency correlations should not be overlooked when modeling price changes at different frequencies.

[2]Specifically, the long-run non-neutrality can be modeled via the *time-to-build* effect (Morley et al., 2003; Grant and Chan, 2017; Li and Mendieta-Muñoz, 2022) and *output hysteresis* (Li and Mendieta-Muñoz, 2024; Furlanetto et al., 2025).

Finally, we point out that, as discussed by Trenkler and Weber (2016) and Li and Mendieta-Muñoz (2022), there exists a set of non-trivial conditions for the identification of multivariate CUC models. In order to understand how the FCUC model is identified, we first highlight that a local level model (Shephard, 2015; Li and Koopman, 2021) leads to an integrated moving average of order 1, IMA(1), reduced-form representation.[3] The latter includes two parameters: the MA coefficient and the innovation variance. Therefore, a bivariate local level model admits a 2-dimensional vector IMA(1) representation with an MA coefficient matrix and a covariance matrix, yielding 7 reduced-form parameters. A constant bivariate FCUC model contains 6 parameters: a factor loading, two correlation coefficients, and three innovation variances, thus satisfying the order condition with an overidentified system.[4]

3.3 Can long-run inflation expectations anchor trend inflation?

It is known that CUC models tend to exacerbate the cross-frequency correlation in finite samples. Morley et al. (2003), Trenkler and Weber (2016), Grant and Chan (2017), and Li and Mendieta-Muñoz (2022) found that the trend-cycle correlation in real GDP is approximately -0.9 with trend (potential) output subject to excess volatility and an uneven path. Moreover, CUC models with a near-perfect (negative) correlation are also counter-intuitive to standard New Keynesian models, as shown by Canova and Ferroni (2022), and can provide poor policy guidance in practice.

One remedy is to connect trend inflation with long-run inflation expectations. Based on the Beveridge-Nelson decomposition (Beveridge and Nelson, 1981), there is an equivalence between trend and long-run rational expectations: $\tau_t = \lim_{s\to\infty} E_t(\pi_{t+s})$. Figure 3 shows our measure of inflation expectations together with sticky, flexible, and aggregate inflation. The inflation expectation series closely tracks the low-frequency behavior of the three inflation series in real time, thus providing an "anchoring effect" that reduces the estimation uncertainty of trend inflation. In section 4.1, we discuss our chosen inflation expectations data.

Faust and Wright (2013) and Chan et al. (2018) considered survey inflation expectations as a regressor in the observation equation of a model similar to (7). They showed that

[3] A local level model is an unobserved components model with a random walk trend and a white noise cycle. In other words, it is the UCSV model in (7) but with constant innovation variances.

[4] In this sense, we could add one extra parameter to incorporate the within-frequency correlation for cycles and obtain exact identification. However, as also discussed above, results from the BUCSV model do not suggest that this is a relevant feature. Hence, we prefer to estimate a more parsimonious model.

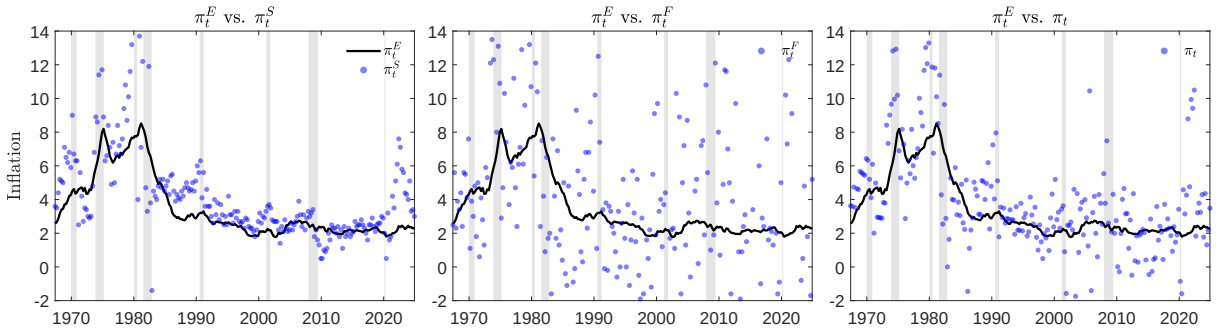

Figure 3: Long-run inflation expectations, sticky inflation, flexible inflation, and aggregate inflation. Long-run inflation expectations (black line) is plotted with sticky inflation (left figure), flexible inflation (middle figure), and aggregate inflation (right figure). Blue dots show the actual values for the different measures of inflation. Our measure of inflation expectation corresponds to the 10-year inflation expectations in Haubrich et al. (2012). Section 4.1 provides further details about the latter. Figures were cropped for readability, with some extreme inflation values outside the range.

incorporating the cointegration between survey inflation expectations and trend inflation into the model greatly reduces model uncertainty. In the same vein, our proposed FCUC model considers inflation expectations π_t^E to load onto the common factor τ_t^C in equation (4) and uses additional information to estimate the local movements of trend inflation.

Since the GFC, inflation expectations have become a focal point of monetary policy, representing both the target and benchmark that measure the effectiveness of forward guidance during periods at the zero lower bound (ZLB) (Harrison, 2015; Sutherland, 2023). As monetary policies discipline agents' expectations (Müller et al., 2022), the latter can also feed back into inflation dynamics via self-fulfilling mechanisms (see, *e.g.*, Harrison, 2015; Angeletos and Lian, 2018; Eusepi et al., 2021). Similar to the multivariate trend-cycle models of Hasenzagl et al. (2022) and Ascari and Fosso (2024), our proposed FCUC model considers an endogenous system for inflation and inflation expectations, and thus allows the expectation formation process to be affected by inflation via β_t with time variation stemming from different economic policies and macroeconomic conditions.

Lastly, we point out that the intercept α_t in the expectation process (4) models potential persistent deviations of agents' expectations from the underlying trend inflation, similar to the specifications in Chan et al. (2018), Hasenzagl et al. (2022) and Comerford (2024). This equation further allows for a stationary adjustment process captured by the MA error ϵ_t^E, analogous to the specification used by Chan et al. (2018).[5]

[5] As in Chan et al. (2018), it is also possible to consider an MA cycle in equations (2) and (3). We considered this

4 Results

This section comprises five parts. Section 4.1 provides a description of the data set employed and motivates the choice of our measure of inflation expectations. Sections 4.2 and 4.3 present a set of estimation results, including the estimates of aggregate trend inflation and other latent processes. A discussion on inflation expectation and its relevance for the FCUC model is provided in section 4.4. Finally, section 4.5 conducts a forecasting performance exercise among variants of the FCUC and UCSV models. We present the posterior estimates of model parameters and the mixing property of the Markov chain in the online appendix.

4.1 Data

Our study uses U.S. quarterly CPI, sticky, and flexible inflation rates, from 1967:Q3 to 2024:Q4 with a total of 231 quarters. The CPI is extracted from the Federal Reserve Bank of St. Louis; whereas the sticky and flexible inflation rates are obtained from the Atlanta Fed following Bryan and Meyer (2010).

As discussed in section 2.2, one crucial time series needed to estimate the proposed FCUC model is the measure of long-run inflation expectations. We adopt the 10-year inflation expectation time series constructed by the Federal Reserve Bank of Cleveland (2022). The series is estimated by an extended model built on Haubrich et al. (2012) that follows a structural no-arbitrage framework and uses an extensive market data set, including inflation swaps and nominal yields. Its market-based construction yields a forward-looking, risk-adjusted measure of long-run inflation expectations that is less susceptible to behavioral biases, liquidity shocks, and sampling issues that are common in surveys (Müller et al., 2022; Hasenzagl et al., 2022; Sutherland, 2023).

Hence, by incorporating real-time pricing and time-varying risk premia, the Cleveland Fed's inflation expectation time series offers increased robustness, particularly during periods of market stress, thus representing a more reliable proxy for long-run inflation expectations.

potential modification, but the estimated coefficients are close to zero with a wide error band. These results are available on request. Because of this, we follow instead the more standard UCSV model specification of Stock and Watson (2007), Shephard (2015) and Li and Koopman (2021) for inflation dynamics.

4.2 Trend inflation and stochastic volatility

Figures 4 and 5 plot the trend inflation estimates obtained from the FCUC model. Specifically, figure 4 shows the posterior estimate of aggregate trend inflation, in comparison to the one obtained from the UCSV model. Figure 5 shows the posterior estimates of the sticky and flexible trend inflation. It also shows the stochastic loading λ_t, since the trends are constructed following equations (2) and (3), where the sticky and flexible trend inflation are equal to the common factor τ_t^C and $\lambda_t \tau_t^C$, respectively.

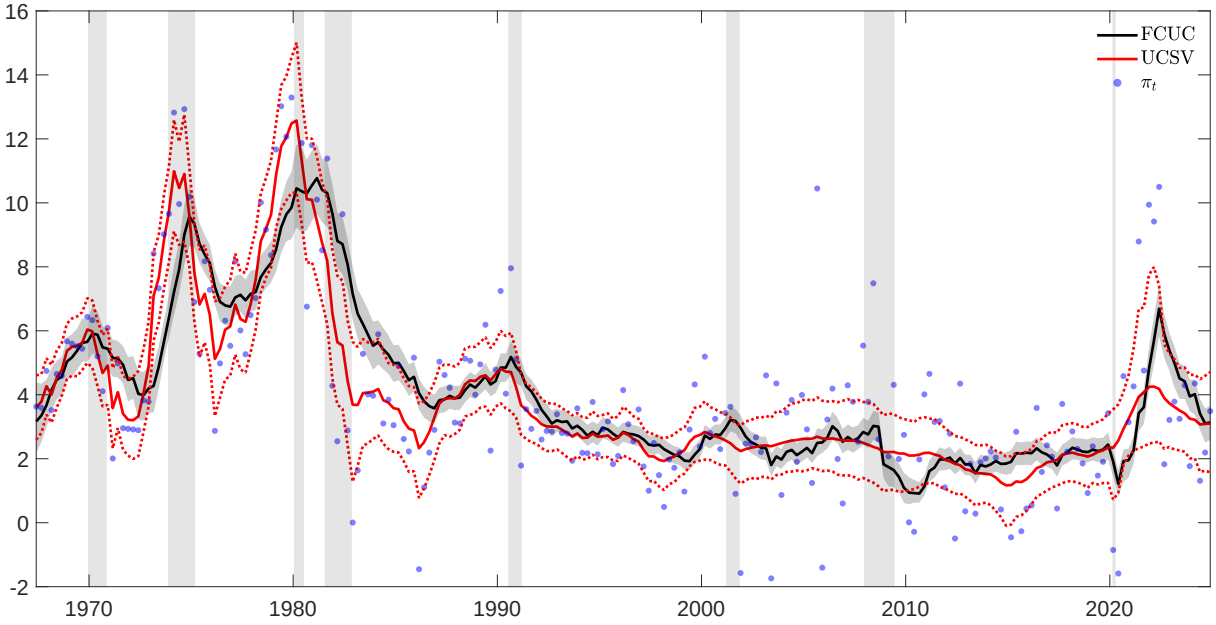

Figure 4: Posterior estimates of the trend inflation obtained from the FCUC and UCSV models. Trend inflation estimates obtained from the FCUC model are constructed following equation (8). Lines show the posterior medians; whereas shaded areas and dotted lines show the $(0.05, 0.95)$ posterior quantiles for each model. Figure is cropped for readability, with some extreme inflation values (blue dots) outside the range.

From figure 4, we see that compared with UCSV, the estimated trend inflation from our FCUC model shows uniformly higher precision, as its error bands tend to be considerably narrower during the whole period. This is due to the estimated positive cross-frequency correlations, as captured by the regression coefficients γ_t and δ_t in (5). Based on (9), we see that the SNR of the FCUC model is always larger than the one of the UCSV model without zero correlation. This can potentially generate excess volatility in trend as in CUC models; however, the presence of both π_t^S and π_t^E largely attenuates the unevenness of the trend estimates. Moreover, the estimated aggregate trend inflation in the FCUC model seems to be mainly derived from τ_t^C,

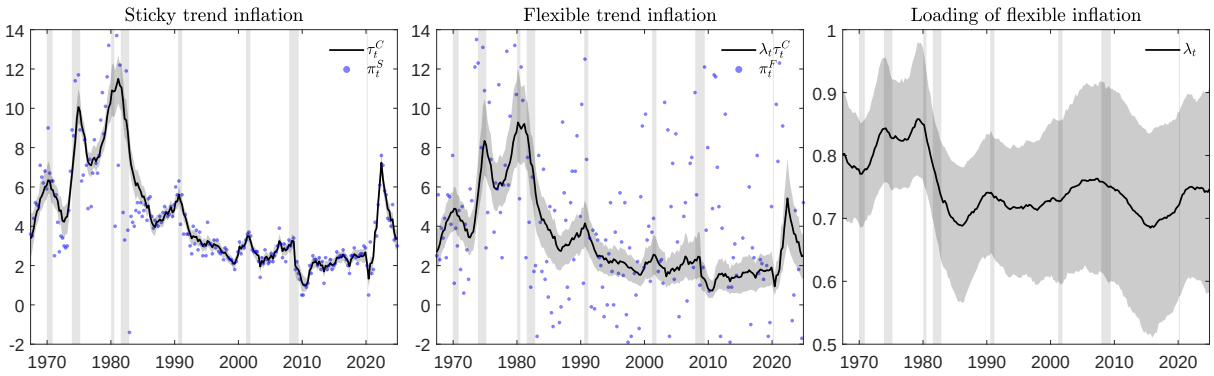

Figure 5: Posterior estimates of the sticky and flexible trend inflation rates obtained the FCUC model. Left to right: sticky trend inflation (common factor) τ_t^C, flexible trend inflation $\lambda_t\tau_t^C$, and time-varying loading of flexible inflation λ_t. Lines show the posterior medians; whereas shaded areas show the $(0.05, 0.95)$ posterior quantiles. Figure is cropped for readability, with some extreme inflation values (blue dots) outside the range.

or the sticky trend. As shown in figure 5, the latter exhibits considerably narrower error bands compared with the flexible trend and its respective time-varying loading λ_t.

The uncertainty in flexible trend is almost solely driven by λ_t, as τ_t^C is precisely estimated. This is not surprising, given the volatile flexible inflation that effects its trend. In the sticky price model of Aoki (2001) and Adam and Weber (2019), this is also anticipated by the largely price-taking behavior of the flexible sector. As a result, Bils and Klenow (2004) argued that flexible inflation contains little forward-looking information. However, in principle, λ_t should fluctuate around one, so that in the long run both sectors index to the same aggregate inflation. Although this contrasts with our finding that λ_t is significantly below one, this argument is less relevant if sectors are heterogeneous and subject to multisector productivity factors, as shown in the menu cost model of Nakamura and Steinsson (2010) and found empirically in the 17-sector factor model of Stock and Watson (2016). Indeed, in the data set of Bryan and Meyer (2010), all inflation items related to housing are considered as flexible, with a distinct productivity factor from sticky sectors such as healthcare and education (Foerster et al., 2022).

To further illustrate the reduced uncertainty of the aggregate trend inflation estimates obtained from the proposed FCUC model, figure 6 shows these estimates only since the GFC and compares them with the ones obtained from the BUCSV and UCSV models, where the latter is fitted to sticky, flexible, and aggregate inflation rates separately.

We observe that the error bands obtained from the FCUC model are clearly narrower compared with the BUCSV and UCSV models. Interestingly, the BUCSV model estimates a flat line for

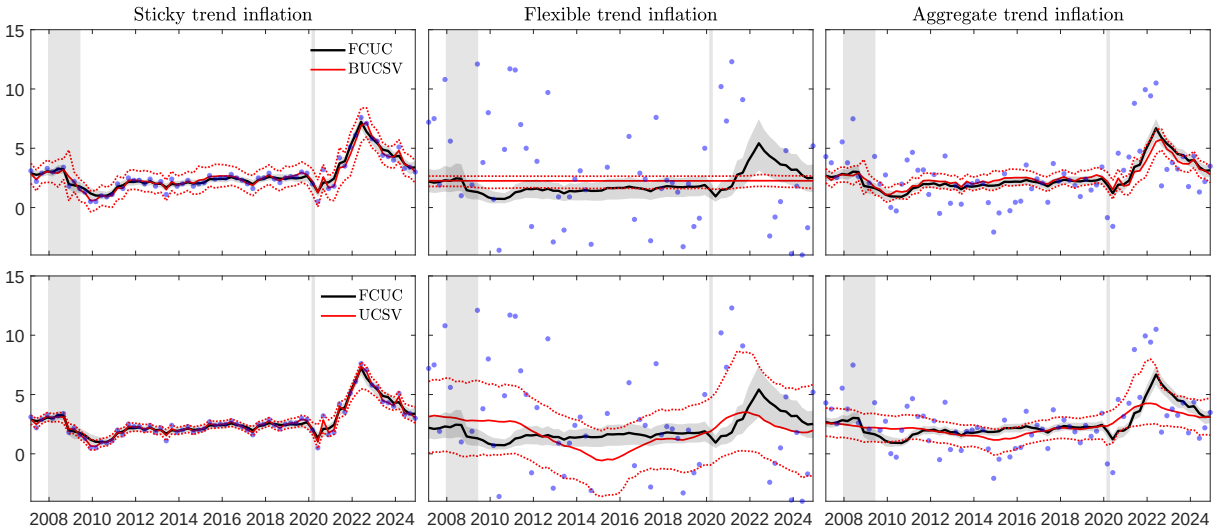

Figure 6: Posterior estimates of the sticky, flexible and aggregate trend inflation rates since the GFC. Left to right: sticky, flexible, and aggregate trend inflation. Top row: FCUC and BUCSV models. Bottom row: FCUC and UCSV models (fitted to sticky, flexible, and aggregate inflation separately). Lines show the posterior medians; whereas shaded areas and dotted lines show the $(0.05, 0.95)$ posterior quantiles for each model. Blue dots show data points.

flexible trend inflation, which does not reflect adequately the relative increase in prices after the COVID-19 recession. Related to the findings shown in figure 1 (bottom right panel), we highlight that the aggregation of sticky and flexible trend inflation estimates obtained from two separate UCSV models results in higher uncertainty for the aggregate trend inflation, especially since the GFC. Lastly, the UCSV model does not reflect either the near-target trend inflation between 2012 and 2019, which was due to well-anchored inflation expectations associated with forward guidance during the initial ZLB period.

4.3 Cross-frequency correlations and variance decomposition

Figure 7 shows the posterior estimates of the stochastic volatility of the sticky and flexible cycles, and the common trend innovation, as specified in equation (6).

We observe significant time variation of both transitory volatility series, whereas the volatility of common trend innovation seems to be largely constant only with a slightly higher value during the first oil crisis of the early 1970s. Notably, the sticky transitory volatility peaks at the second oil crisis in the early 1980s but only mildly rises during the first one in 1974. Following the Great Moderation, it plummets when the flexible transitory volatility quickly picks up the heightened economic uncertainty during the 2001, GFC, and COVID-19 recessions. Importantly, different

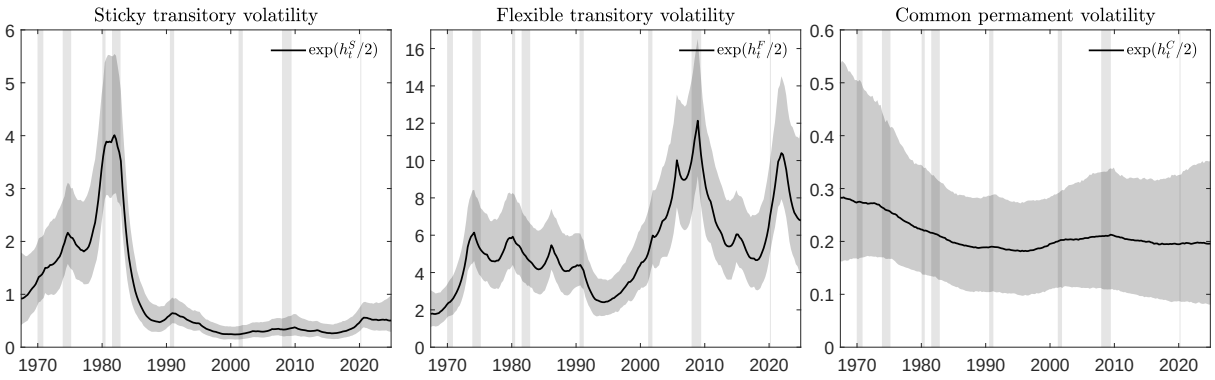

Figure 7: Posterior estimates of the stochastic volatility components obtained from the FCUC model. Left to right: sticky transitory volatility, flexible transitory volatility, and common permanent volatility. Lines show the posterior medians; whereas shaded areas show the $(0.05, 0.95)$ posterior quantiles.

from the permanent volatility obtained from the UCSV model, shown in the top left panel of figure 1, the sticky transitory volatility is precisely estimated during the pandemic. The fact that it is the increase in flexible volatility the one that drives the aggregate inflation uncertainty foreshadows our later discussion about the role of transitory shocks in driving trend inflation.

Given the unique behaviors of the three volatility series, figure 8 shows their implications for the permanent and transitory volatility and persistence of the aggregate inflation: (i) the aggregate permanent volatility σ_t^τ, summarized by (9); (ii) the aggregate transitory volatility, given by $\sqrt{\omega_s^2 \exp(h_t^S) + \omega_F^2 \exp(h_t^F)}$; and (iii) the SNR, *i.e.*, the permanent-to-transitory volatility ratio that measures inflation persistence in UCSV models. We also compare these results with the ones obtained from the UCSV model fit to aggregate inflation.

We find that the transitory volatility of both models resembles each other, with the one obtained from the UCSV model slightly underestimating cyclical fluctuations during the 1970s-80s and, thus, attributing higher volatility to the trend. As a result, the UCSV model's permanent volatility is significantly higher during these two decades and presents much wider error bands during the estimation period. Importantly, the UCSV model does not capture meaningfully any increase in permanent volatility in the wake of the COVID-19 recession, so it does not help to understand whether or not price changes are persistent. On the contrary, the FCUC model greatly sharpens the permanent volatility estimate with a much narrower error band. As the dynamic discounting feature of UCSV models relies on the estimates of permanent and transitory volatility, more accurately estimated volatility components in the

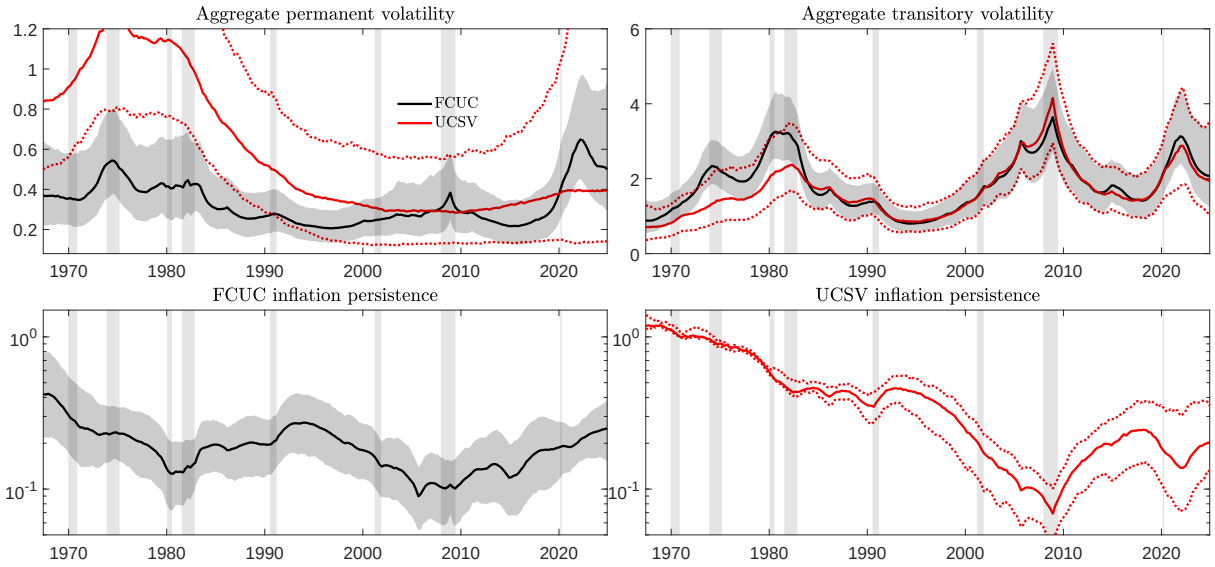

Figure 8: Aggregate permanent volatility, aggregate transitory volatility, and inflation persistence. Top row: Aggregate permanent and transitory volatility components obtained from the FCUC and UCSV models. Bottom row (y-axis in log scale): implied inflation persistence measured by the SNR. Lines show the posterior medians; whereas shaded areas and dotted lines show the $(0.05, 0.95)$ posterior quantiles for each model. The top left figure is cropped for readability. The UCSV's model permanent and transitory volatility components are also reported in figure 1.

FCUC model can better distinguish between permanent shifts in inflation from transitory movements.

Both Lansing (2022) and Jørgensen and Lansing (2024) discuss that the SNR is directly related to the correlation coefficient between consecutive changes in the level of inflation and, therefore, it can be regarded as a measure of inflation persistence. This conceptualization is closely related to the "memory index" of Shephard (2015), who showed that the number of periods that a rational agent would look back to predict inflation in the next period is inversely related to the SNR. In other words, both contributions highlight that, when the SNR is high (low), changes in inflation are more (less) likely to be persistent.

The SNR obtained from both models, illustrated in the bottom panel of figure 8, shows a similar gradual decrease until the GFC and an increase afterwards. However, due to the high uncertainty in the permanent volatility of aggregate inflation at the beginning of the COVID-19 recession, the UCSV model fails to accurately capture the increasing inflation persistence, which is better captured by our FCUC model (see also Ball et al., 2022 and Lansing, 2022 for a discussion). Overall, these dynamics almost mirror the behavior of inflation itself, which has been heavily influenced by changes in monetary policy—with the Volcker disinflation of the early

1980s serving as the example *par excellence*. Hence, our findings provide evidence in favor of monetary non-neutrality (Nakamura and Steinsson, 2010), the view that measures of inflation persistence can be influenced by shifts in monetary policy itself (Daly, 2022), and reveal that inflation dynamics have become more persistent since the GFC.

Figure 9 shows the time-varying cross-frequency correlation between the sticky (flexible) inflation cycle and the common factor innovation component, summarized by the coefficient ρ_t^{CS} (ρ_t^{CF}) in (10). The bottom panel of figure 9 also shows the variance decomposition of the aggregate trend inflation obtained from the FCUC model.

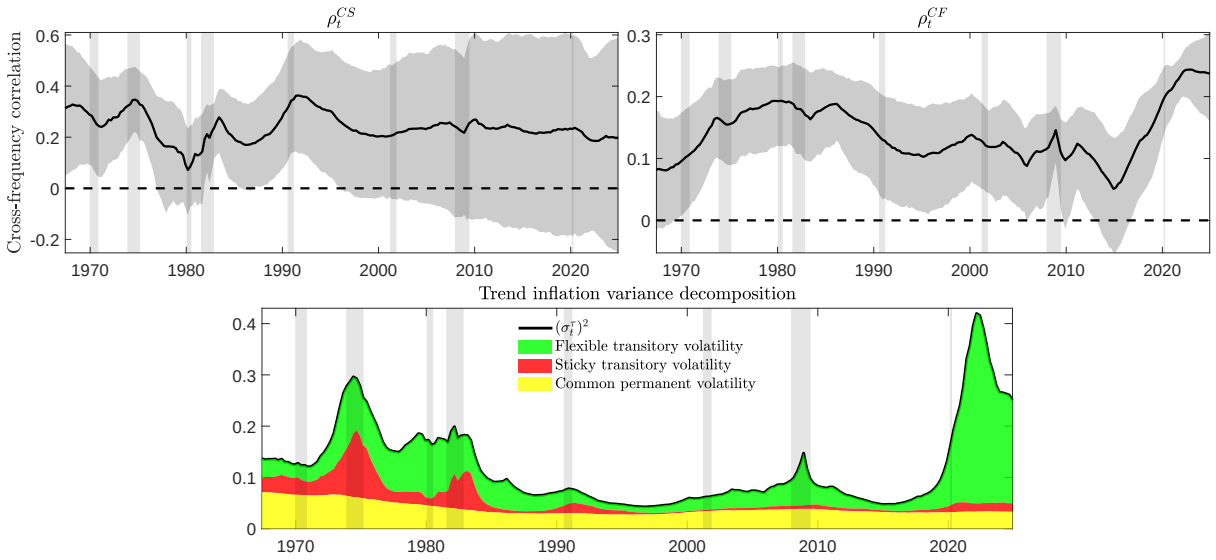

Figure 9: Cross-frequency correlations and variance decomposition of the aggregate trend inflation obtained from the FCUC model. Top row: ρ_t^{CS} (left figure) and ρ_t^{CF} (right figure) as depicted by equation (10). Lines show the posterior medians; whereas shaded areas show the $(0.05, 0.95)$ posterior quantiles. Bottom row: variance decomposition based on equation (9).

This exercise demonstrates that, while transitory volatility can drive fluctuations in trend inflation during recessions, its impact depends on the source of price shocks and is not time invariant. In the first half of the sample, amid the two oil crises, the sticky cycle effects importantly trend inflation, explaining 50% of its variation, 20% more than flexible cycle shocks. This reflects the combined effect of a positive cross-frequency correlation and elevated sticky-cycle volatility, or ρ_t^{CS} and h_t^S, respectively. In the second half of the period, the relative importance of these components shifts markedly: with ρ_t^{CS} no longer significantly different from zero, the contribution of the sticky cycle to trend inflation declines rapidly following the Great Moderation; while flexible price shocks emerge as the dominant driver and account for

90% of trend variation, particularly during the COVID-19 recession. Although Ball et al. (2022) and Dao et al. (2024) suggest that headline shocks have only recently passed through to core inflation, we find that the rising correlation between flexible shocks and common trend innovations predates the pandemic and substantially contributed to the 2020-2 inflation surge.

Importantly, the volatility of the common trend inflation innovation, or the permanent component h_t^C, remains largely stable and accounts for 60% of trend inflation fluctuations in the 1990s when flexible price shocks were subdued, but only 10% in recent periods. This highlights the growing influence of relative price shocks on trend inflation and the policy challenges they pose. In the context of optimal monetary policy under macroeconomic uncertainty, Alvarez and Lippi (2020), Gopinath (2022) and Bernanke and Blanchard (2024) caution against the complications that large relative price shocks introduce for both level and average inflation targeting, due to monetary non-neutrality arising from their spillovers into core inflation. Our results quantify the time-varying strength of this spillover and challenge the view of Aoki (2001) that central banks should focus solely on sticky or core inflation. We believe that our findings suggest that this conventional approach can break down importantly during sharp recessions when the assumption of flexible sectors as the only passive price takers no longer holds (see also Nakamura and Steinsson, 2010, Lafuente et al., 2021 and Rubbo, 2024). In light of interacting trend inflation and multisector price shocks, it becomes essential for central banks to move beyond conventional core inflation metrics and consider alternative welfare-maximizing targets (Nakamura and Steinsson, 2010; Adam and Weber, 2019), such as those defined by nominal distortions—see, *e.g.*, Eusepi et al. (2011), Stock and Watson (2020), and Coulombe et al. (2024).

4.4 The relevance of long-run inflation expectations

Figure 10 shows the posterior estimates of α_t and β_t, that is, the time-varying intercept and time-varying factor loading, respectively, associated with the inflation expectation equation (4). Similar to Chan et al. (2018) and Hasenzagl et al. (2022), α_t in our FCUC model captures the potential persistent deviations of inflation expectations from trend inflation; while β_t is a regression coefficient that connects both series.

The results show that the evolution of α_t has been stable, approximately around 2% during the

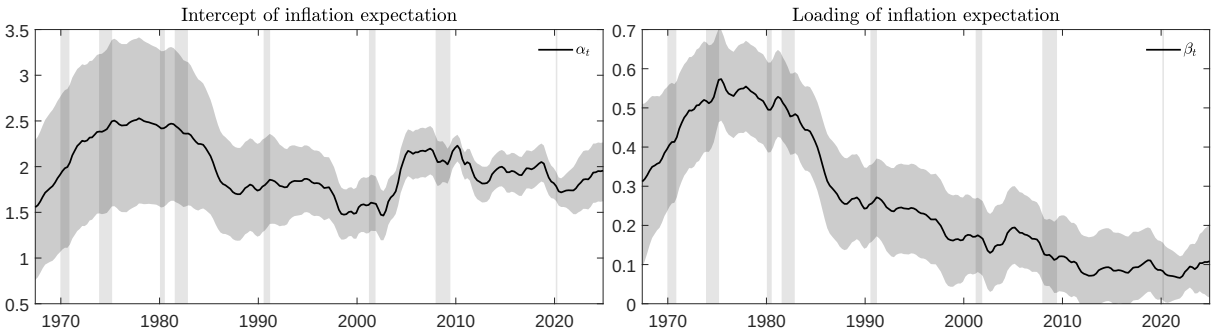

Figure 10: Time-varying intercept and factor loading of inflation expectations obtained from the FCUC model. The time-varying intercept α_t (left figure) and time-varying loading β_t (right figure) of inflation expectations are shown in equation (4). Lines and shaded areas show the posterior medians and $(0.05, 0.95)$ quantiles, respectively.

period, with an inverted-U shape and wider error bands during the 1970s-80s, followed by greater stability and narrower bands thereafter. This evolution is consistent with better anchoring amid the Volcker-Greenspan-Bernanke regimes and the introduction of inflation targeting that followed. By contrast, β_t exhibits a similar inverted-U pattern early on but declines noticeably afterwards. Additionally, it remains positive but consistently below one, indicating that changes in sticky trend inflation exert only limited influence on expectations and *vice versa*. These results suggest persistent deviations from rational expectations, a finding similar to Chan et al. (2018) and Hasenzagl et al. (2022), who used survey-based expectations.

To assess the importance of including inflation expectations in the FCUC model, figure 11 reports the cross-frequency correlations, trend inflation, and permanent volatility estimates obtained from the FCUC model excluding π_t^E by omitting equation (4). The estimates of the other latent variables are fairly similar and therefore are omitted.

Including the long-run inflation expectations equation visibly reduces the posterior error bands in the FCUC model, thus reducing estimation uncertainty. Although the cross-frequency correlation between the flexible inflation cycle and the common factor, ρ_t^{CF}, remains broadly similar with or without expectations (top right panel of figure 11), omitting π_t^E leads to an inflated estimate of the transitory influence from sticky inflation, as shown by a much larger ρ_t^{CS} (top left panel of figure 11). This mirrors the well-known trend-cycle identification issue in CUC models, where the correlation coefficient can approach unity in absolute value due to a small sample bias (Morley et al., 2003; Wada, 2012; Li and Mendieta-Muñoz, 2024). In our setting, the omission of π_t^E leads to an overestimated SNR, evident in both the higher

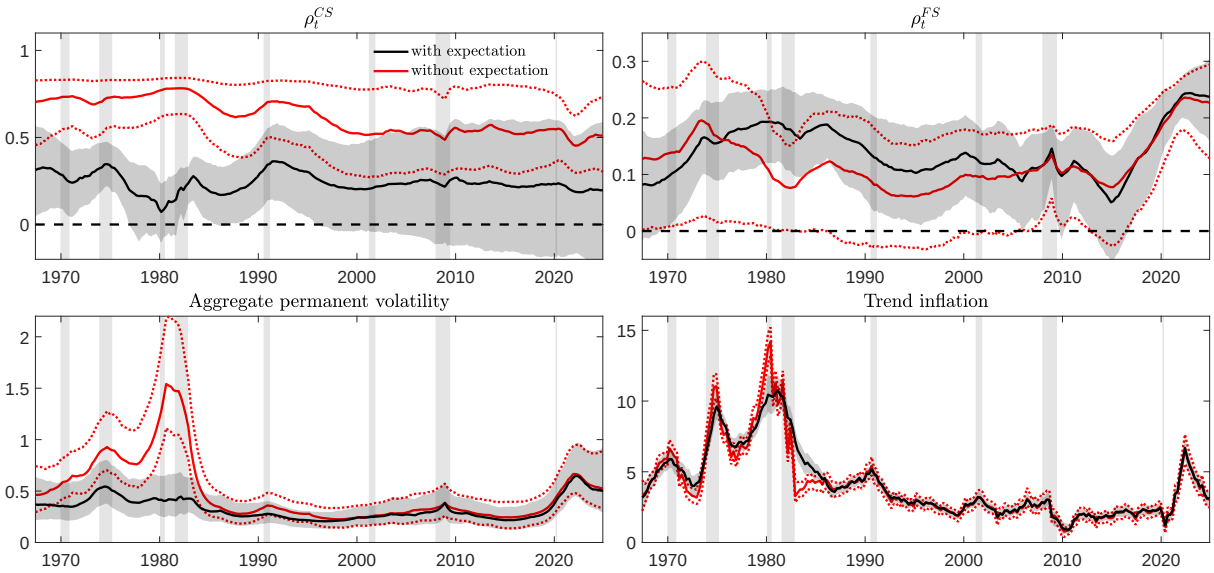

Figure 11: Posterior estimates obtained from the FCUC model with and without the inflation expectations equation (4). Black and red lines show the posterior estimates of the FCUC model with inflation expectations and without inflation expectations, respectively. Lines show the posterior medians; whereas shaded areas and dotted lines show the $(0.05, 0.95)$ posterior quantiles for each model.

aggregate permanent volatility σ_t^τ (bottom left panel) and the more erratic trend inflation path (bottom right panel), especially prior to the Great Moderation.

By contrast, incorporating π_t^E into the FCUC model improves identification via an expanded information set, allowing long-run expectations to load directly onto the common factor and thereby mitigating the inflated correlation problem. Unlike traditional factor models that rely on large cross-sectional data (Bai and Ng, 2008), our model gains precision with minimal added noise, as the error variance in ϵ_t^E remains small (see the online appendix). As a result, the FCUC model with π_t^E offers an intuitive yet robust decomposition of inflation dynamics, assigning clearer roles to the underlying unobserved components. In this sense, our model is easily scalable due to the factor structure. Future research may explore broader information sets that include measures of economic slack and granular sectoral inflation series to help understand the emergence and transmission of flexible price shocks.

4.5 Forecasting performance

To assess what model features can generalize the observed inflation data, we compare the out-of-sample forecasting performance of the FCUC model and some of its variants with UCSV models,

focusing on the last two decades of major economic downturns. We use an expanding window design with the first training sample covering the period 1967:Q3-2006:Q4.[6] Then, all models are re-estimated with the sample moved one quarter ahead. We consider h-quarters ahead forecasts, where $h \in \{1, 2, 3, 4\}$. The full testing sample covers the period 2007:Q1-2024:Q4, the same as in figure 6, which gives us 72 and 69 forecast errors for each model under $h = 1$ and $h = 4$, respectively. We use the root mean squared errors (RMSE) and log predictive density scores (LPDS) to evaluate point and density forecast, respectively. Models with lower RMSE and higher LPDS are preferred.

Besides the proposed FCUC model, we consider nine competing models, which can be grouped into three classes. First, simple models include: (i) a random walk (RWalk) model; (ii) a model that only uses sticky inflation data to forecast (Sticky); and (iii) the expectation-in-gap-form (ExG) model of Faust and Wright (2013) which, despite its simplicity, is "amazingly hard to beat by much," as mentioned by the authors (p. 17).[7] Second, UCSV models include: (i) the original model of Stock and Watson (2007); (ii) the ExG-TVP model of Chan et al. (2018) that extends the ExG model by considering a random walk trend inflation plus MA(1) dynamics for long-run inflation expectations, a time-varying AR coefficient for the inflation cycle, and stochastic volatility components for both the inflation trend and cycle; and (iii) the BUCSV model of Eo et al. (2023) that we modified to incorporate sticky and flexible inflation. Third, FCUC models include: (i) the FCUC model without long-run inflation expectations (FCUC-noEx); (ii) the FCUC model with constant cross-frequency correlation coefficients (FCUC-cCr); and (iii) the FCUC model without cross-frequency correlation coefficients (FCUC-noCr).[8]

Main results are reported in table 1. The RWalk model performs worst across all horizons, reflecting its inability to accommodate large swings during the GFC and the COVID-19 pandemic. Surprisingly, the Sticky model consistently outperforms the ExG model, despite the latter's AR(1) cycle, which suggests that sticky inflation captures more accurately shifts in inflation dynamics than long-run inflation expectations alone. Additionally, the ExG-TVP

[6] A rolling window design yields nearly identical results. The latter is available upon request.

[7] In the ExG model, trend inflation is fixed at the survey long-run inflation expectations level and the inflation cycle is modeled as an autoregressive (AR) process of order 1.

[8] All models are estimated via Bayesian methods except for the three simple models. The forecast is the posterior mean: $\int g(\pi_{t+h}) p(\pi_{t+h}|D_m, \boldsymbol{\theta}_m) p(\boldsymbol{\theta}_m|D_m) d\boldsymbol{\theta}_m$, where D_m denotes the training data set of model m with a vector of model parameters $\boldsymbol{\theta}_m$. For the RMSE, $g(\pi_{t+h}) = \pi_{t+h}$ is simulated from the model of interest. For the LPDS, $g(\pi_{t+h}) = 1$ is used to evaluate the density ordinate of the observed h-quarter ahead inflation. The integral is replaced by an average in which 10^5 samples of $\boldsymbol{\theta}_m$ are drawn from $p(\boldsymbol{\theta}_m|D_m)$.

Table 1: Point and density forecast accuracy of models

	RMSE				LPDS			
	$h=1$	$h=2$	$h=3$	$h=4$	$h=1$	$h=2$	$h=3$	$h=4$
Simple models								
RWalk	3.690	4.148	4.091	4.295	−2.850	−2.901	−2.908	−2.995
Sticky	3.122	3.197	3.281	3.397	—	—	—	—
ExG	3.245	3.459	3.434	3.542	−2.706	−2.719	−2.691	−2.718
UCSV models								
UCSV	**3.070**	3.194	3.230	3.296	−2.414	−2.473	−2.552	−2.587
ExG-TVP	3.105	3.164	3.223	**3.241**	−2.988	−2.982	−2.988	−2.855
BUCSV	3.115	3.172	3.233	3.290	**−2.403**	−2.460	−2.542	−2.551
FCUC models								
FCUC	3.082	**3.146**	**3.205**	**3.266**	**−2.409**	**−2.449**	**−2.536**	**−2.542**
FCUC-noEx	**3.067**	**3.133**	**3.212**	3.280	−2.414	−2.458	**−2.536**	**−2.547**
FCUC-noCr	3.188	3.215	3.244	3.290	−2.444	−2.503	−2.568	−2.573
FCUC-cCr	3.149	3.192	3.226	3.275	−2.423	**−2.456**	−2.545	−2.552

Notes: Forecast accuracy is evaluated at one- through four-quarter horizons using root mean squared errors (RMSE) for point forecasts and log predictive density scores (LPDS) for density forecasts. Out-of-sample forecasts cover the period 2007:Q1-2024:Q4, with model parameters re-estimated recursively using expanding windows beginning in 1967:Q2. Bold numbers indicate the two best models.

model outperforms the ExG model, thus indicating the importance of modeling time-varying dynamics for the generalization of the inflation process. At $h = 4$, the ExG-TVP model yields the lowest RMSE, followed closely by the FCUC model, which suggests some evidence of mean reversion at longer horizons. At $h = 1$, the UCSV model performs best, followed closely by the FCUC-noEx model. This result indicates that, for short-run forecasting, parsimonious models with dynamic discounting that stems from trend and cycle stochastic volatility are preferred (Shephard, 2015; Lansing, 2022). Also, the gains derived from incorporating long-run inflation expectations emerge at longer horizons, which can be seen by the relative improvement in the performance of the FCUC model, thus supporting the view that expectations help to anchor trend inflation (Chan et al., 2018; Hasenzagl et al., 2022; Müller et al., 2022). Lastly, we highlight that the FCUC models, with and without long-run inflation expectations, rank among the top performers, indicating that cross-frequency correlations and their time variation capture inflation dynamics robustly, and that their exclusion affects RMSE more than omitting long-run expectations.

For density forecasts at $h = 1$, the FCUC model ranks second and yields a slightly lower LPDS than the BUCSV model (while other models are much lower). The main feature in both models is the highly positive correlation between sticky and flexible trend inflation that feeds into the aggregate trend inflation. Therefore, the modeling of overlapping trends seem to provide a better conditional central tendency and, consequently, a more accurate predictive coverage during periods of economic distress. The FCUC model turns out to be the best density forecaster for all $h > 1$, closely followed by the FCUC-noEx and FCUC-cCr models. This ranking clarifies that both long-run inflation expectations and the time variation in cross-frequency correlations improve the predictive coverage, especially the latter, as suggested by the LPDS at $h > 2$.

Finally, we test for equal predictive ability among model pairs, excluding simple models, using the Diebold–Mariano test (Diebold and Mariano, 1995; Diebold, 2015), with the small-sample correction of Harvey et al. (1997). Results are shown in table 2, which reports test statistics based on squared error differentials (point forecasts) and LPDS differentials (density forecasts).

Due to the limited testing sample size and volatile inflation environment, we do not find numerous significant rejections of the null hypothesis of equal predictive performance. Nevertheless, three findings are noticeable. First, FCUC models differ significantly from UCSV models in point forecasts for $h > 1$; while for $h = 1$ only the FCUC-noCr model shows a significant difference. Given the FCUC-noCr model's higher RMSE and absence of richer trend-cycle dynamics, this supports our earlier conclusion that parsimony benefits mainly short-run forecasting. Second, FCUC models differ from UCSV models in density forecasts across all horizons, thus indicating that the inclusion of inflation components, long-run inflation expectations, and cross-frequency correlations enhances predictive coverage. Third, for density forecasts within the class of FCUC models, the FCUC-noEx model tends to differ from the FCUC-noCr and FCUC-cCr models at most horizons, but only from the FCUC model at $h = 1$. This highlights that the time-varying cross-frequency correlation is a key driver of predictive gains, and implies that the evolving long-run spillovers from sticky and flexible prices in the last two decades complicate the policy makers' assessment of trend inflation and should be explicitly accounted for in econometric models.

In sum, the above results show that, while UCSV models benefit from dynamic discounting, the proposed FCUC model improves out-of-sample generalizability through structural

Table 2: Tests for equal predictive ability of models

	UCSV	ExG-TVP	BUCSV	FCUC-noEx	FCUC	FCUC-noCr	FCUC-cCr
$h = 1$							
UCSV	—	1.19	1.00	1.81*	1.66*	0.88	2.13**
ExG-TVP	0.43	—	2.59**	2.28**	2.12**	2.68**	2.42**
BUCSV	1.91*	1.66*	—	1.37	1.91*	1.16	1.19
FCUC-noEx	0.78	1.20	1.83*	—	1.66*	2.80**	0.93
FCUC	1.61	0.67	0.39	2.34**	—	3.02**	1.80*
FCUC-noCr	2.01**	0.71	1.62	4.71**	2.49**	—	3.04**
FCUC-cCr	1.30	0.67	1.65*	2.58**	0.48	2.02**	—
$h = 2$							
UCSV	—	1.91*	0.79	1.35	1.69*	0.77	1.82*
ExG-TVP	0.93	—	2.25**	2.03**	2.11**	2.21**	2.04*
BUCSV	2.30**	1.09	—	0.67	2.13**	2.16**	1.78*
FCUC-noEx	1.62*	1.24	0.14	—	1.12	3.25**	1.14
FCUC	1.87*	1.78*	0.63	1.19	—	3.36**	1.92*
FCUC-noCr	1.92*	0.65	0.77	3.32**	2.60**	—	4.33**
FCUC-cCr	2.04**	2.02**	0.94	2.96**	1.38	0.78	—
$h = 3$							
UCSV	—	1.89*	0.72	1.99**	1.69*	1.14	1.83*
ExG-TVP	1.88*	—	2.67**	2.41**	2.41**	2.41**	2.30**
BUCSV	2.59**	2.28**	—	1.54	2.00**	2.29**	1.67*
FCUC-noEx	1.38	0.71	0.60	—	1.63	0.72	2.26**
FCUC	1.65*	0.80	1.83*	4.25**	—	3.34**	1.86*
FCUC-noCr	1.98**	0.83	1.16	0.19	0.83	—	2.12**
FCUC-cCr	1.61	1.76*	1.80*	0.31	0.80	2.14**	—
$h = 4$							
UCSV	—	1.79*	1.17	1.65*	1.89*	0.73	1.84*
ExG-TVP	2.54**	—	2.48**	2.22**	2.10**	2.27**	2.26**
BUCSV	0.96	1.93*	—	2.16**	1.68*	2.63**	1.74*
FCUC-noEx	0.55	0.23	0.78	—	1.28	1.95*	1.35
FCUC	0.07	0.34	1.90*	1.89*	—	5.80**	2.30**
FCUC-noCr	0.01	0.61	1.31	1.13	1.92*	—	4.23**
FCUC-cCr	0.14	0.61	1.40	2.09**	1.41	1.82*	—

Notes: We report the absolute t-statistics obtained from the Diebold–Mariano test (Diebold and Mariano, 1995; Diebold, 2015) with the finite-sample correction of Harvey et al. (1997). We compare models pairs indicated by rows and columns. One and two asterisks denote rejection of equal predictive ability at the 10% and 5% levels, respectively. For each forecast horizon, the lower- and upper-triangular part of the table show the test results based on loss differentials for squared forecast errors (point forecasts) and log predictive density scores (density forecasts), respectively.

heterogeneity and cross-frequency dynamics, especially during periods of heightened volatility.

5 Summary and conclusion

This paper develops a factor correlated unobserved components (FCUC) model that jointly estimates the trend and cycle dynamics of the sticky and flexible components of U.S. inflation. By incorporating stochastic volatility, stochastic loadings, time-varying cross-frequency correlations, and long-run inflation expectations, the model generalizes existing unobserved components frameworks to better reflect heterogeneity in price adjustment and the effect of transitory shocks on trend inflation. The proposed FCUC model is estimated for the period 1967:Q3-2024:Q4 using Bayesian methods. The results show that, flexible inflation, traditionally considered as being driven by transitory and policy irrelevant relative price shocks, has strongly affected trend inflation. This spillover begins to emerge around 2015 and becomes particularly pronounced during the COVID-19 recession, while sticky inflation, comprising purely persistent price shocks since 1980s, accounts for only part of the aggregate trend dynamics.

These findings show the importance of accounting for the evolving interactions between high- and low-frequency disaggregated components of inflation when evaluating inflation persistence. From a policy perspective, the presence of cross-frequency correlation challenges the argument that transitory price movements warrant little policy response as they have short-lived aggregate effects (see, *e.g.*, Aoki, 2001, Alvarez and Lippi, 2020, Powell, 2021, and Lansing, 2022). By contrast, our analysis supports Ball et al. (2022), Gopinath (2022) and Bernanke and Blanchard (2024) in the aftermath of the COVID-19 pandemic: while large price shocks in flexible prices (such as food and energy prices) accounted for much of the initial inflation surge, we cannot rule out monetary tightening due to their persistent effects on aggregate inflation. Overall, our results suggest that monetary authorities should not disregard temporary price fluctuations, particularly in flexible price components, as these can heavily influence long-run inflation and expectations formation, an idea emphasized by earlier studies including Nakamura and Steinsson (2010) and Eusepi et al. (2011). The proposed FCUC framework thus offers a robust tool for improving trend inflation measurement and informing forward-looking policy decisions.

References

Adam, K. and H. Weber (2019). Optimal trend inflation. *American Economic Review 109*(2), 702–737.

Alvarez, F. and F. Lippi (2020). Temporary price changes, inflation regimes, and the propagation of monetary shocks. *American Economic Journal: Macroeconomics 12*(1), 104–152.

Angeletos, G.-M. and C. Lian (2018). Forward guidance without common knowledge. *American Economic Review 108*(9), 2477–2512.

Aoki, K. (2001). Optimal monetary policy responses to relative-price changes. *Journal of monetary economics 48*(1), 55–80.

Ascari, G. and L. Fosso (2024). The international dimension of trend inflation. *Journal of International Economics 148*, 103896.

Bai, J. and S. Ng (2008). Large dimensional factor analysis. *Foundations and Trends® in Econometrics 3*(2), 89–163.

Ball, L., D. Leigh, and P. Mishra (2022). Understanding US inflation during the COVID-19 era. *Brookings Papers on Economic Activity 2022*(2), 1–80.

Bernanke, B. and O. Blanchard (2024). An analysis of pandemic-era inflation in 11 economies. *Peterson Institute for International Economics Working Paper*, 24–11.

Beveridge, S. and C. R. Nelson (1981). A new approach to decomposition of economic time series into permanent and transitory components with particular attention to measurement of the 'business cycle'. *Journal of Monetary Economics 7*(2), 151–174.

Bils, M. and P. J. Klenow (2004). Some evidence on the importance of sticky prices. *Journal of Political Economy 112*(5), 947–985.

Bitto, A. and S. Frühwirth-Schnatter (2019). Achieving shrinkage in a time-varying parameter model framework. *Journal of Econometrics 210*(1), 75–97.

Bryan, M. F. and B. Meyer (2010). Are some prices in the CPI more forward looking than others? We think so. *Economic Commentary* (2010-02).

Canova, F. and F. Ferroni (2022). Mind the gap! Stylized dynamic facts and structural models. *American Economic Journal: Macroeconomics 14*(4), 104–135.

Carvalho, A., J. V. e Azevedo, and P. P. Ribeiro (2024). Permanent and temporary monetary policy shocks and the dynamics of exchange rates. *Journal of International Economics 147*, 103871.

Chan, J. C. (2017). The stochastic volatility in mean model with time-varying parameters: An application to inflation modeling. *Journal of Business & Economic Statistics 35*(1), 17–28.

Chan, J. C., T. E. Clark, and G. Koop (2018). A new model of inflation, trend inflation, and long-run inflation expectations. *Journal of Money, Credit and Banking 50*(1), 5–53.

Chan, J. C. and I. Jeliazkov (2009). Efficient simulation and integrated likelihood estimation in state space models. *International Journal of Mathematical Modelling and Numerical Optimisation 1*(1-2), 101–120.

Comerford, D. A. (2024). Response bias in survey measures of expectations: Evidence from the survey of consumer expectations' inflation module. *Journal of Money, Credit and Banking 56*(4), 933–953.

Coulombe, P. G., K. Klieber, C. Barrette, and M. Göbel (2024). Maximally forward-looking core inflation. *arXiv preprint arXiv:2404.05209*.

Daly, M. C. (2022). This time is different...Because we are. *FRBSF Economic Letter* (05). Accessed May 2025.

Dao, M. C., P.-O. Gourinchas, D. Leigh, and P. Mishra (2024). Understanding the international rise and fall of inflation since 2020. *Journal of Monetary Economics 148*, 103658.

Diebold, F. X. (2015). Comparing predictive accuracy, twenty years later: A personal perspective on the use and abuse of Diebold–Mariano tests. *Journal of Business & Economic Statistics 33*(1), 1–1.

Diebold, F. X. and R. S. Mariano (1995). Comparing predictive accuracy. *Journal of Business & Economic Statistics 13*(3), 253–263.

Eo, Y., L. Uzeda, and B. Wong (2023). Understanding trend inflation through the lens of the goods and services sectors. *Journal of Applied Econometrics 38*(5), 751–766.

Eusepi, S., C. Gibbs, and B. Preston (2021). Forward guidance with unanchored expectations. *Bank of Finland Research Discussion Papers*, 11.

Eusepi, S., B. Hobijn, and A. Tambalotti (2011). CONDI: A cost-of-nominal-distortions index. *American Economic Journal: Macroeconomics 3*(3), 53–91.

Faust, J. and J. H. Wright (2013). Forecasting inflation. In *Handbook of Economic Forecasting*, Volume 2, pp. 2–56. Elsevier.

Federal Reserve Bank of Cleveland (2022, August). Inflation expectations. Federal Reserve Bank of Cleveland. https://doi.org/10.26509/frbc-infexp. Accessed May 2025.

Foerster, A. T., A. Hornstein, P.-D. G. Sarte, and M. W. Watson (2022). Aggregate implications of changing sectoral trends. *Journal of Political Economy 130*(12), 3286–3333.

Furlanetto, F., A. Lepetit, Ø. Robstad, J. Rubio-Ramírez, and P. Ulvedal (2025). Estimating hysteresis effects. *American Economic Journal: Macroeconomics 17*(1), 35–70.

Gopinath, G. (2022, August). How will the pandemic and war shape future monetary policy? Remarks at the Jackson Hole Economic Policy Symposium. https://www.imf.org/en/News/Articles/2022/08/26/sp-gita-gopinath-remarks-at-the-jackson-hole-symposium. Accessed May 2025.

Grant, A. L. and J. C. Chan (2017). A Bayesian model comparison for trend-cycle decompositions of output. *Journal of Money, Credit and Banking 49*(2-3), 525–552.

Harrison, R. (2015). Estimating the effects of forward guidance in rational expectations models. *European Economic Review 79*, 196–213.

Harvey, D., S. Leybourne, and P. Newbold (1997). Testing the equality of prediction mean squared errors. *International Journal of Forecasting 13*(2), 281–291.

Hasenzagl, T., F. Pellegrino, L. Reichlin, and G. Ricco (2022). A model of the Fed's view on inflation. *Review of Economics and Statistics 104*(4), 686–704.

Haubrich, J., G. Pennacchi, and P. Ritchken (2012). Inflation expectations, real rates, and risk premia: Evidence from inflation swaps. *Review of Financial Studies 25*(5), 1588–1629.

Hofmann, B., C. Manea, and B. Mojon (2024). Targeted Taylor rules: monetary policy responses to demand-and supply-driven inflation. *BIS Quarterly Review*, 19.

Hwu, S. T. and C. J. Kim (2019). Estimating trend inflation based on unobserved components model: is it correlated with the inflation gap? *Journal of Money, Credit and Banking 51*(8), 2305–2319.

Imbs, J., E. Jondeau, and F. Pelgrin (2011). Sectoral Phillips curves and the aggregate Phillips curve. *Journal of Monetary Economics 58*(4), 328–344.

Jordá, O., C. Marti, and F. Nechio (2022). Why is U.S. inflation higher than in other countries? *FRBSF Economic Letter* (03). Accessed May 2025.

Jørgensen, P. L. and K. J. Lansing (2024). Anchored inflation expectations and the slope of the Phillips curve. *Federal Reserve Bank of San Francisco Working Paper 27*.

Kim, S., N. Shephard, and S. Chib (1998). Stochastic volatility: likelihood inference and comparison with ARCH models. *Review of Economic Studies 65*(3), 361–393.

Lafuente, J. Á., M. Monfort, R. Pérez, and J. Ruiz (2021). Disentangling permanent and transitory monetary shocks with a nonlinear Taylor rule. *Economics 15*(1), 150–162.

Lansing, K. J. (2022). Untangling persistent versus transitory shocks to inflation. *FRBSF Economic Letter 13*.

Lenza, M. and G. E. Primiceri (2022). How to estimate a vector autoregression after March 2020. *Journal of Applied Econometrics 37*(4), 688–699.

Li, M. and S. J. Koopman (2021). Unobserved components with stochastic volatility: Simulation-based estimation and signal extraction. *Journal of Applied Econometrics 36*(5), 614–627.

Li, M. and I. Mendieta-Muñoz (2022). Bayesian analysis of structural correlated unobserved components and identification via heteroskedasticity. *Studies in Nonlinear Dynamics & Econometrics 26*(3), 337–359.

Li, M. and I. Mendieta-Muñoz (2024). Dynamic hysteresis effects. *Journal of Economic Dynamics and Control 163*, 104870.

Morley, J. C., C. R. Nelson, and E. Zivot (2003). Why are the Beveridge-Nelson and unobserved-components decompositions of GDP so different? *Review of Economics and Statistics 85*(2), 235–243.

Müller, T., K. Christoffel, F. Mazelis, and C. Montes-Galdón (2022). Disciplining expectations and the forward guidance puzzle. *Journal of Economic Dynamics and Control 137*, 104336.

Nakamura, E. and J. Steinsson (2010). Monetary non-neutrality in a multisector menu cost model. *The Quarterly journal of economics 125*(3), 961–1013.

Powell, J. H. (2021, August). Monetary policy in the time of COVID. Speech at the Economic Policy Symposium, Jackson Hole, sponsored by the Federal Reserve Bank of Kansas City. https://www.federalreserve.gov/newsevents/speech/files/powell20210827a.pdf. Accessed May 2025.

Rubbo, E. (2024). What drives inflation? Lessons from disaggregated price data. *NBER Working Paper* (w32194).

Shapiro, A. H. (2024). Decomposing supply-and demand-driven inflation. *Journal of Money, Credit and Banking forthcoming*.

Shephard, N. (2015). Martingale unobserved component models. In S. J. Koopman and N. Shephard (Eds.), *Unobserved Components and Time Series Econometrics*, pp. Chapter

10. Oxford University Press.

Stock, J. H. and M. W. Watson (2007). Why has US inflation become harder to forecast? *Journal of Money, Credit and Banking 39*, 3–33.

Stock, J. H. and M. W. Watson (2016). Core inflation and trend inflation. *Review of Economics and Statistics 98*(4), 770–784.

Stock, J. H. and M. W. Watson (2020). Slack and cyclically sensitive inflation. *Journal of Money, Credit and Banking 52*(S2), 393–428.

Sutherland, C. S. (2023). Forward guidance and expectation formation: A narrative approach. *Journal of Applied Econometrics 38*(2), 222–241.

Trenkler, C. and E. Weber (2016). On the identification of multivariate correlated unobserved components models. *Economics Letters 138*, 15–18.

Wada, T. (2012). On the correlations of trend–cycle errors. *Economics Letters 116*(3), 396–400.

Unpacking trend inflation: Evidence from a factor correlated unobserved components model of sticky and flexible prices — Online appendix

Mengheng Li*

Ivan Mendieta-Muñoz†

July 4, 2025

This online appendix accompanies: Li, Mengheng, and Mendieta-Muñoz, Ivan. (2025). "*Unpacking trend inflation: Evidence from a factor correlated unobserved components model of sticky and flexible prices*". We provide details of the Bayesian estimation procedure for the factor correlated unobserved components (FCUC) model, introduced in section 2 of the main text. We also report the relevant mixing statistics of the Markov chain that fits the FCUC model to our data set, which consists of sticky and flexible inflation rates and a measure of long-run inflation expectations. This appendix provides only supporting materials and it is not meant for publication. Notations follow the main text, unless stated otherwise.

Keywords: trend inflation; sticky inflation; flexible inflation; stochastic volatility; dynamic factor model.

JEL Classification: C32; C53; E37.

*Senior Lecturer (Assistant Professor). University of Technology Sydney (UTS) Business School and Centre for Applied Macroeconomic Analysis (CAMA). Email: mengheng.li@uts.edu.au

†Associate Professor. Department of Economics, University of Utah. Email: ivan.mendietamunoz@utah.edu

1 Sampling procedure

The MCMC sampler iterates over the following three major blocks:

- Sample model parameters $\boldsymbol{\theta} = (\sigma_g, \phi)$, $g \in \{h^S, h^F, h^C, E, \alpha, \beta, \lambda, \gamma, \delta\}$, conditional on latent states and initializations, or $(\boldsymbol{\theta}|\boldsymbol{\pi}, \boldsymbol{f}, f_0)$, where $f = \{h^S, h^F, h^C, \tau^C, \alpha, \beta, \lambda, \gamma, \delta\}$;
- Sample latent states conditional on model parameters and initializations, or $(\boldsymbol{f}|\boldsymbol{\pi}, f_0, \boldsymbol{\theta})$;
- Sample initializations conditional on model parameters and latent states, or $(f_0|\boldsymbol{\pi}, \boldsymbol{f}, \boldsymbol{\theta})$.

In the description of the sampling procedure above, $\boldsymbol{\pi} = \left((\boldsymbol{\pi}^S)', (\boldsymbol{\pi}^F)', (\boldsymbol{\pi}^E)'\right)'$ collects the data, where bold fonts indicate the vector of a time series variable, *e.g.*, $\boldsymbol{\pi}^S = (\pi_1^S, ..., \pi_T^S)'$.

1.1 Sample model parameters

Sample variances

Let the gamma prior in section 2.3 of the main text be denoted by $\sigma_g^2 \sim \Gamma(a, b)$ with prior

$$p_0(\sigma_g^2) \propto (\sigma_g^2)^{a-1} \exp(-b\sigma_g^2). \tag{1}$$

For σ_f^2, we have

$$\boldsymbol{H}\boldsymbol{f} = \boldsymbol{e}_1 f_0 + \boldsymbol{\epsilon}^f, \quad \boldsymbol{\epsilon}^f \sim N(\boldsymbol{0}, \sigma_f^2 \boldsymbol{I}_T),$$

where $\boldsymbol{I}_T$ is a $T \times T$ identity matrix, $\boldsymbol{e}_s$ is the s-th unit vector in $\mathbb{R}^T$, and $\boldsymbol{H}$ is a $T \times T$ matrix that first differences $\boldsymbol{f}$, or

$$\boldsymbol{H} = \begin{bmatrix} 1 & 0 & 0 & \cdots & 0 \\ -1 & 1 & 0 & \cdots & 0 \\ 0 & -1 & 1 & \cdots & 0 \\ \vdots & \vdots & \ddots & \ddots & \vdots \\ 0 & 0 & \cdots & -1 & 1 \end{bmatrix}.$$

This yields the conditional likelihood

$$p(\boldsymbol{f}|\sigma_f^2, f_0) \propto (\sigma_f^2)^{-\frac{T}{2}} \exp\left(-\frac{1}{2\sigma_f^2} \tilde{\boldsymbol{f}}' \boldsymbol{H}' \boldsymbol{H} \tilde{\boldsymbol{f}}\right), \tag{2}$$

where $\tilde{\boldsymbol{f}} = \boldsymbol{f} - \boldsymbol{H}^{-1}\boldsymbol{e}_1 f_0 = \boldsymbol{f} - \boldsymbol{1} f_0$, and $\boldsymbol{1}$ is a vector of ones. Combining the likelihood (2)

with the prior (1), we can derive

$$p(\sigma_f^2|\boldsymbol{f}, f_0) \propto (\sigma_f^2)^{-\frac{T}{2}-a} \exp\left(-\frac{\tilde{\boldsymbol{f}}'\boldsymbol{H}'\boldsymbol{H}\tilde{\boldsymbol{f}}}{2\sigma_f^2} + 2b\sigma_f^2\right).$$

This is the kernel of the generalized inverse Gaussian (GIG) distribution. We follow Eisenstat et al. (2016) and sample the variance parameters as follows:

$$\sigma_f^2|\boldsymbol{f}, f_0 \sim GIG\left(a - \frac{T}{2}, 2b, \tilde{\boldsymbol{f}}'\boldsymbol{H}'\boldsymbol{H}\tilde{\boldsymbol{f}}\right)$$

for $f = \{h^S, h^F, h^C, \alpha, \beta, \lambda, \gamma, \delta\}$.

To sample σ_E^2, we use equation (4) in the main text. We write the latter in matrix form:

$$\begin{aligned} \tilde{\boldsymbol{\pi}}^E &= \boldsymbol{H}_\phi \boldsymbol{\epsilon}^E, \quad \boldsymbol{\epsilon}^E \sim N(\boldsymbol{0}, \sigma_E^2 \boldsymbol{I}_T), \\ \tilde{\boldsymbol{\pi}}^E &= \boldsymbol{\pi}^E - \boldsymbol{\alpha} - \boldsymbol{\beta} \odot \boldsymbol{\pi}^C, \end{aligned} \tag{3}$$

where $\odot$ indicates element-by-element product, and

$$\boldsymbol{H}_\phi = \begin{bmatrix} 1 & 0 & 0 & \cdots & 0 \\ -\phi & 1 & 0 & \cdots & 0 \\ 0 & -\phi & 1 & \cdots & 0 \\ \vdots & \vdots & \ddots & \ddots & \vdots \\ 0 & 0 & \cdots & -\phi & 1 \end{bmatrix}.$$

Following (2), the conditional likelihood in this case is

$$p(\boldsymbol{\pi}^E|\sigma_E^2, \boldsymbol{\alpha}, \boldsymbol{\beta}, \phi) \propto (\sigma_E^2)^{-\frac{T}{2}} \exp\left(-\frac{1}{2\sigma_E^2}(\tilde{\boldsymbol{\pi}}^E)'(\boldsymbol{H}_\phi \boldsymbol{H}_\phi')^{-1}\tilde{\boldsymbol{\pi}}^E\right).$$

Combing it with the prior (1) gives the conditional posterior

$$p(\sigma_E^2|\boldsymbol{\pi}^E, \boldsymbol{\alpha}, \boldsymbol{\beta}, \phi) \propto (\sigma_E^2)^{-\frac{T}{2}-a} \exp\left(-\frac{(\tilde{\boldsymbol{\pi}}^E)'(\boldsymbol{H}_\phi \boldsymbol{H}_\phi')^{-1}\tilde{\boldsymbol{\pi}}^E}{2\sigma_E^2} + 2b\sigma_E^2\right).$$

We sample from the following GIG distribution:

$$\sigma_E^2|\boldsymbol{\pi}^E, \boldsymbol{\alpha}, \boldsymbol{\beta}, \phi \sim GIG\left(a - \frac{T}{2}, 2b, (\tilde{\boldsymbol{\pi}}^E)'(\boldsymbol{H}_\phi \boldsymbol{H}_\phi')^{-1}\tilde{\boldsymbol{\pi}}^E\right).$$

Sample MA coefficient

Using (3), we have the conditional likelihood

$$p(\boldsymbol{\pi}^E|\sigma_E^2, \boldsymbol{\alpha}, \boldsymbol{\beta}, \phi) \propto \exp\left(-\frac{1}{2\sigma_E^2}(\tilde{\boldsymbol{\pi}}^E)'(\boldsymbol{H}_\phi \boldsymbol{H}_\phi')^{-1}\tilde{\boldsymbol{\pi}}^E\right),$$

such that the gamma prior (1) is not conjugate. We implement a standard Metropolis-Hastings step. Let $\hat{\phi}$ and $\widehat{\text{Var}}(\hat{\phi})$ denote the mean and variance, respectively, of the Laplace approximation (denoted by $\sim^*$, meaning approximate distribution up to location and scale),

$$\phi|\boldsymbol{\pi}^E, \sigma_E^2, \boldsymbol{\alpha}, \boldsymbol{\beta} \sim^* N\big(\hat{\phi}, \widehat{\text{Var}}(\hat{\phi})\big), \tag{4}$$

where the parameters are defined by:

$$\begin{aligned}
\hat{\phi} &= \arg\max_\phi \left[\log p(\boldsymbol{\pi}^E|\sigma_E^2, \boldsymbol{\alpha}, \boldsymbol{\beta}, \phi) + \log p_0(\phi)\right], \\
\widehat{\text{Var}}(\hat{\phi}) &= -\left(\frac{\partial^2}{(\partial\phi)^2}\left[\log p(\boldsymbol{\pi}^E|\sigma_E^2, \boldsymbol{\alpha}, \boldsymbol{\beta}, \phi) + \log p_0(\phi)\right]\Big|_{\phi=\hat{\phi}}\right)^{-1},
\end{aligned}$$

where $p_0(\phi)$ is the truncated normal prior for the MA coefficient defined in section 2.3 of the main text.

We generate a draw ϕ^{new} from the approximate distribution (4). Let ϕ^{old} denote the current draw in the Markov chain and let $N(x; u, v)$ denote the density ordinate of a normal distribution with mean u and variance v evaluated at x. The draw is accepted with probability

$$\min\left[\frac{p(\boldsymbol{\pi}^E|\sigma_E^2, \boldsymbol{\alpha}, \boldsymbol{\beta}, \phi^{\text{new}})p_0(\phi^{\text{new}})N(\phi^{\text{old}}; \hat{\phi}, \widehat{\text{Var}}(\hat{\phi}))}{p(\boldsymbol{\pi}^E|\sigma_E^2, \boldsymbol{\alpha}, \boldsymbol{\beta}, \phi^{\text{old}})p_0(\phi^{\text{old}})N(\phi^{\text{new}}; \hat{\phi}, \widehat{\text{Var}}(\hat{\phi}))}, 1\right],$$

otherwise $\phi^{\text{new}} = \phi^{\text{old}}$.

1.2 Sample latent states

Sample common trend $\boldsymbol{\tau}^C$

In brief, to sample $\boldsymbol{\tau}^C$ is to sample $\boldsymbol{\epsilon}^S$. First, we notice that

$$\pi_t^f = \lambda_t(\pi_t^S - \epsilon_t^S) + \epsilon_t^F. \tag{5}$$

Similarly, we rewrite the equation for the inflation expectations, or equation (4) in the main text:

$$\pi_t^E - \alpha_t = \beta_t(\pi_t^S - \epsilon_t^S) + \epsilon_t^E + \theta\epsilon_t^E,$$

which yields

$$\underbrace{\hat{\pi}_t^E}_{\pi_t - \alpha_t - \beta_t\pi_t^S} = -\beta_t\epsilon_t^S + \epsilon_t^E + \theta\epsilon_t^E. \tag{6}$$

Using (5) to replace ϵ_t^F in the transition dynamics of the common trend, or equation (5) in the main text, we have

$$\begin{aligned}\tau^C &= \tau_{t-1}^C + \gamma_t\epsilon_t^S + \delta_t(\pi_t^F - \lambda_t\pi_t^S + \lambda_t\epsilon_t^S) + \eta_t^C \\ &= \tau_{t-1}^C + \underbrace{\delta_t(\pi_t^F - \lambda_t\pi_t^S)}_{z_t} + \underbrace{(\gamma_t + \delta_t\lambda_t)\epsilon_t^S}_{x_t} + \eta_t^C.\end{aligned} \tag{7}$$

In matrix form, equation (7) becomes

$$\boldsymbol{H}\boldsymbol{\tau}^C = \boldsymbol{e}_1\tau_0^C + \boldsymbol{z} + \boldsymbol{x} \odot \boldsymbol{\epsilon}^S + \boldsymbol{\eta}^C.$$

Combining the equation above with $\boldsymbol{H}\boldsymbol{\pi}^S = \boldsymbol{H}\boldsymbol{\tau}^S + \boldsymbol{H}\boldsymbol{\epsilon}^S$ (that is, pre-multiplying $\boldsymbol{H}$ to equation (2) in the main text) yields

$$\boldsymbol{H}\boldsymbol{\tau}^S = \boldsymbol{e}_1\tau_0^C + \boldsymbol{z} + (\text{diag}(\boldsymbol{x}) + \boldsymbol{H})\boldsymbol{\epsilon}^S + \boldsymbol{\eta}^C, \tag{8}$$

where $\text{diag}(\boldsymbol{y})$ denotes a diagonal matrix of the same dimension as the vector $\boldsymbol{y}$ whose elements also form the diagonal elements of the matrix. Casting equation (3) in matrix form yields

$$\hat{\boldsymbol{\pi}}^E = \text{diag}(-\boldsymbol{\beta})\boldsymbol{\epsilon}^S + \boldsymbol{H}_\phi\boldsymbol{\epsilon}^E. \tag{9}$$

Putting (8) and (9) together yields

$$\underbrace{\begin{pmatrix} \boldsymbol{H}\boldsymbol{\pi}^S - \boldsymbol{e}_1\tau_0^C - \boldsymbol{z} \\ \boldsymbol{H}_\phi^{-1}\hat{\boldsymbol{\pi}}^E \end{pmatrix}}_{\boldsymbol{\pi}^*} = \underbrace{\begin{bmatrix} \text{diag}(\boldsymbol{x}) + \boldsymbol{H} \\ \boldsymbol{H}_\phi^{-1}\text{diag}(-\boldsymbol{\beta}) \end{bmatrix}}_{\boldsymbol{X}} \boldsymbol{\epsilon}^S + \underbrace{\begin{pmatrix} \boldsymbol{\eta}^C \\ \boldsymbol{\epsilon}^E \end{pmatrix}}_{\boldsymbol{\epsilon}^*}, \quad \boldsymbol{\epsilon}^*|\boldsymbol{h}^C, \sigma_E^2 \sim N(\boldsymbol{0}, \boldsymbol{\Sigma}),$$

where

$$\boldsymbol{\Sigma} = \begin{bmatrix} \text{diag}(\exp^\bullet(\boldsymbol{h}^C)) & \boldsymbol{O} \\ \boldsymbol{O} & \sigma_E^2 \boldsymbol{I}_T \end{bmatrix},$$

$\exp^\bullet(.)$ denotes element-wise exponential and $\boldsymbol{O}$ is a $T \times T$ matrix of zeros. Using the Bayesian regression lemma (where $\boldsymbol{\pi}^*$ is the vector of responses and $\boldsymbol{X}$ is the matrix of regressors), we have the conditional posterior

$$\boldsymbol{\epsilon}^S|\boldsymbol{\pi}, \boldsymbol{\lambda}, \boldsymbol{\alpha}, \boldsymbol{\beta}, \boldsymbol{\delta}, \boldsymbol{\gamma}, \boldsymbol{h}^C, \boldsymbol{h}^S, \phi, \sigma_E^2 \sim N(\boldsymbol{\mu}_C, \boldsymbol{P}_C^{-1}),$$

where

$$\boldsymbol{P}_C = \exp^\bullet(-\boldsymbol{h}^S) + \boldsymbol{X}'\boldsymbol{\Sigma}^{-1}\boldsymbol{X},$$
$$\boldsymbol{\mu}_C = \boldsymbol{P}_C^{-1}\boldsymbol{X}'\boldsymbol{\Sigma}^{-1}\boldsymbol{\pi}^*.$$

Since all the matrices involved in the derivation above are tri-diagonal, we use the fast precision sampler of Chan and Jeliazkov (2009) to sample from the above multivariate Gaussian conditional posterior, utilizing efficient routines of sparse matrix inversion and Cholesky decomposition that are available in Matlab® 2022b.

Sample loading $\boldsymbol{\lambda}$

It is instrumental to notice that we cannot sample λ_t directly from the flexible inflation equation (3) in the main text, conditional on τ_t^C. This is so because τ_t^C and the innovation term (flexible cycle) η_t^F are correlated, or $E(\boldsymbol{\tau}^C(\boldsymbol{\eta}^F)'|\boldsymbol{\gamma}, \boldsymbol{\delta}) \neq \boldsymbol{O}$, which is an endogeneity issue that requires us to first de-correlate them for correct posterior inference.

We write equation (3) in the main text in matrix form:

$$\begin{aligned}\boldsymbol{\pi}^F &= \boldsymbol{\tau}^C \odot \boldsymbol{\lambda} + \boldsymbol{\epsilon}^F \\ &= \boldsymbol{\nu} + \text{diag}(\boldsymbol{\tau}^C)\boldsymbol{\lambda} + \tilde{\boldsymbol{\eta}}^F, \quad \tilde{\boldsymbol{\eta}}^F | \boldsymbol{h}^F, \boldsymbol{h}^C m\boldsymbol{\delta} \sim N(\mathbf{0}, \boldsymbol{\Sigma}^F),\end{aligned} \tag{10}$$

where $\boldsymbol{\nu}$ and $\boldsymbol{\Sigma}^F$ is the conditional mean and covariance of $\boldsymbol{\epsilon}^F$ (conditional on $\boldsymbol{\tau}^C$). To derive these, we write the transition equation of the common trend in matrix form:

$$\boldsymbol{H}\boldsymbol{\tau}^C = \boldsymbol{e}_1\tau_0^C + \boldsymbol{\gamma} \odot \boldsymbol{\epsilon}^S + \text{diag}(\boldsymbol{\delta})\boldsymbol{\epsilon}^F + \boldsymbol{\eta}^C, \quad \boldsymbol{\eta}^C | \boldsymbol{h}^C \sim N(\mathbf{0}, \text{diag}(\exp^\bullet(\boldsymbol{h}^C))), \tag{11}$$

which is a regression on $\boldsymbol{\eta}^F$. Given the conditional prior $\boldsymbol{\eta}^F | \boldsymbol{h}^F \sim N(\mathbf{0}, \text{diag}(\exp^\bullet(\boldsymbol{h}^F)))$, we can compute the conditional mean and covariance matrix using the Bayesian regression lemma as follows:

$$\begin{aligned}\left(\boldsymbol{\Sigma}^F\right)^{-1} &= \text{diag}(\exp^\bullet(-\boldsymbol{h}^F)) + \text{diag}(\boldsymbol{\delta})'\text{diag}(\exp^\bullet(-\boldsymbol{h}^C))\text{diag}(\boldsymbol{\delta}) \\ \boldsymbol{\nu} &= \boldsymbol{\Sigma}^F \text{diag}(\boldsymbol{\delta})'\text{diag}(\exp^\bullet(-\boldsymbol{h}^C))(\boldsymbol{H}\boldsymbol{\tau}^C - \boldsymbol{e}_1\tau_0^C - \boldsymbol{\gamma} \odot \boldsymbol{\epsilon}^S).\end{aligned}$$

With the equation above determined, we go back to equation (10), which is a regression on $\boldsymbol{\lambda}$. Based on the conditional prior $\boldsymbol{\lambda}|\lambda_0, \sigma_\lambda^2 \sim N(\mathbf{1}\lambda_0, \sigma_\lambda^2(\boldsymbol{H}'\boldsymbol{H})^{-1})$ derived from $\boldsymbol{H}\boldsymbol{\lambda} = \boldsymbol{e}_1\lambda_0 + \boldsymbol{\epsilon}^\lambda$ with $\boldsymbol{\epsilon}^\lambda | \sigma_\lambda^2 \sim N(\mathbf{0}, \sigma_\lambda^2 \boldsymbol{I}_T)$, using the Bayesian regression lemma we obtain

$$\boldsymbol{\lambda} | \boldsymbol{\pi}^F, \boldsymbol{\pi}^S, \boldsymbol{\tau}^C, \boldsymbol{\gamma}, \boldsymbol{\delta}, \boldsymbol{h}^C, \boldsymbol{h}^F, \sigma_\lambda^2, \lambda_0 \sim N(\boldsymbol{\mu}_\lambda, \boldsymbol{P}_\lambda^{-1}),$$

where

$$\begin{aligned}\boldsymbol{P}_\lambda &= \frac{1}{\sigma_\lambda^2}(\boldsymbol{H}'\boldsymbol{H}) + \text{diag}(\boldsymbol{\tau}^C)'(\boldsymbol{\Sigma}^F)^{-1}\text{diag}(\boldsymbol{\tau}^C), \\ \boldsymbol{\mu}_\lambda &= \boldsymbol{P}_\lambda^{-1}\left(\frac{\lambda_0}{\sigma_\lambda^2}\boldsymbol{H}'\boldsymbol{e}_1 + \text{diag}(\boldsymbol{\tau}^C)'(\boldsymbol{\Sigma}^F)^{-1}(\boldsymbol{\tau}^F - \boldsymbol{v})\right).\end{aligned}$$

Sample regression coefficients γ and δ

We rewrite (11) as a regression on $\boldsymbol{\gamma}$ and $\boldsymbol{\delta}$. It follows that

$$\underbrace{\boldsymbol{H}\boldsymbol{\tau}^C - \boldsymbol{e}_1\tau_0^C}_{\hat{\boldsymbol{\pi}}^C} = \underbrace{\text{diag}(((\boldsymbol{\epsilon}^S)', (\boldsymbol{\epsilon}^F)')')}_{\boldsymbol{X}_\epsilon} \begin{pmatrix} \boldsymbol{\gamma} \\ \boldsymbol{\delta} \end{pmatrix} + \boldsymbol{\eta}^C, \quad \boldsymbol{\eta}^C|\boldsymbol{h}^C \sim N(\boldsymbol{0}, \text{diag}(\exp^\bullet(\boldsymbol{h}^C))).$$

Given the conditional prior

$$\begin{pmatrix} \boldsymbol{\gamma} \\ \boldsymbol{\delta} \end{pmatrix} \Big| \gamma_0, \delta_0, \sigma_\gamma^2, \sigma_\delta^2 \sim N\left((\gamma_0, \delta_0)' \otimes \boldsymbol{1}, (\sigma_\gamma^2, \sigma_\delta^2)' \otimes (\boldsymbol{H}'\boldsymbol{H})^{-1}\right),$$

using the Bayesian regression lemma leads to the following conditional posterior:

$$\begin{pmatrix} \boldsymbol{\gamma} \\ \boldsymbol{\delta} \end{pmatrix} \Big| \boldsymbol{\pi}^S, \boldsymbol{\pi}^F, \boldsymbol{\tau}^C, \boldsymbol{\lambda}, \boldsymbol{h}^C, \sigma_\gamma^2, \sigma_\delta^2, \gamma_0, \delta_0 \sim N(\boldsymbol{\mu}_{\gamma,\delta}, \boldsymbol{P}_{\gamma,\delta}^{-1}),$$

where

$$\begin{aligned} \boldsymbol{P}_{\gamma,\delta} &= \left(\frac{1}{\sigma_\gamma^2}, \frac{1}{\sigma_\delta^2}\right)' \otimes (\boldsymbol{H}'\boldsymbol{H}) + \boldsymbol{X}_\epsilon' \text{diag}(\exp^\bullet(-\boldsymbol{h}^C))\boldsymbol{X}_\epsilon, \\ \boldsymbol{\mu}_{\gamma,\delta} &= \boldsymbol{P}_{\gamma,\delta}^{-1}\left(\left(\frac{\gamma_0}{\sigma_\gamma^2}, \frac{\delta_0}{\sigma_\delta^2}\right)' \otimes \boldsymbol{H}'\boldsymbol{e}_1 + \boldsymbol{X}_\epsilon' \text{diag}(\exp^\bullet(-\boldsymbol{h}^C))\hat{\boldsymbol{\pi}}^C\right). \end{aligned}$$

Sample regression coefficients α and β

We rewrite (3) as a regression on $\boldsymbol{\alpha}$ and $\boldsymbol{\beta}$. It follows that

$$\boldsymbol{\pi}^E = \underbrace{\text{diag}((\boldsymbol{1}', (\boldsymbol{\tau}^C)')')}_{\boldsymbol{X}_E} \begin{pmatrix} \boldsymbol{\alpha} \\ \boldsymbol{\beta} \end{pmatrix} + \tilde{\epsilon}^E, \quad \tilde{\epsilon}^E|\phi, \sigma_E^2 \sim N(\boldsymbol{0}, \sigma_E^2(\boldsymbol{H}_\phi \boldsymbol{H}_\phi')).$$

Given the conditional prior

$$\begin{pmatrix} \boldsymbol{\alpha} \\ \boldsymbol{\beta} \end{pmatrix} \Big| \sigma_\alpha^2, \sigma_\beta^2, \alpha_0, \beta_0 \sim N\left((\alpha_0, \beta_0)' \otimes \boldsymbol{1}, (\sigma_\alpha^2, \sigma_\beta^2)' \otimes (\boldsymbol{H}'\boldsymbol{H})^{-1}\right),$$

using the Bayesian regression lemma leads to the following conditional posterior:

$$\begin{pmatrix} \boldsymbol{\alpha} \\ \boldsymbol{\beta} \end{pmatrix} \Big| \boldsymbol{\pi}^E, \boldsymbol{\tau}^C, \phi, \boldsymbol{h}^C, \sigma_E^2, \sigma_\alpha^2, \sigma_\beta^2, \alpha_0, \beta_0 \sim N(\boldsymbol{\mu}_{\alpha,\beta}, \boldsymbol{P}_{\alpha,\beta}^{-1}),$$

where

$$\begin{aligned} \boldsymbol{P}_{\alpha,\beta} &= \left(\frac{1}{\sigma_\alpha^2}, \frac{1}{\sigma_\beta^2}\right)' \otimes (\boldsymbol{H}'\boldsymbol{H}) + \frac{1}{\sigma_E^2} \boldsymbol{X}'_E (\boldsymbol{H}_\phi \boldsymbol{H}'_\phi)^{-1} \boldsymbol{X}_E, \\ \boldsymbol{\mu}_{\alpha,\beta} &= \boldsymbol{P}_{\alpha,\beta}^{-1} \left(\left(\frac{\alpha_0}{\sigma_\alpha^2}, \frac{\beta_0}{\sigma_\beta^2}\right)' \otimes \boldsymbol{H}'\boldsymbol{e}_1 + \frac{1}{\sigma_E^2} \boldsymbol{X}'_E (\boldsymbol{H}_\phi \boldsymbol{H}'_\phi)^{-1} \hat{\boldsymbol{\pi}}^E \right). \end{aligned}$$

Sample stochastic volatility $\boldsymbol{h}^m$, $m \in \{S, F, C\}$

With the aforementioned latent states sampled, we obtain $\boldsymbol{\eta}^m$, $m \in \{S, F, C\}$, which are sufficient statistics for the log volatility $\boldsymbol{h}^m$. Let $\boldsymbol{\kappa}^m = (\log[(\eta_1^m)^2], ..., \log[(\eta_T^m)^2])'$. We suppress the superscript for presentation. Then, equation (6) in the main text becomes

$$\boldsymbol{\kappa} = \boldsymbol{I}_T \boldsymbol{h} + \boldsymbol{\zeta}, \tag{12}$$

where $\boldsymbol{\zeta} = (\zeta_1, ..., \zeta_T)'$ with ζ_t being the logarithm of the square of standard Gaussian innovation terms. Specifically, ζ_t is log-χ^2 distributed with one degree of freedom. We follow Kim et al. (1998) and approximate the nonstandard distribution by using a 7-component Gaussian mixture via data augmentation:

$$\zeta_t \approx \sum_{i=1}^{7} \mathbb{1}_{\{q_t = i\}} N(\nu_i, v_i),$$

where ν_i and v_i are tabulated by Kim et al. (1998), and the prior probabilities of the mixing component $q_t \in \{1, ..., 7\}$ are also tabulated and given by

$$P(q_t = i) = q_i, \quad i = 1, ..., 7,$$

with $q_i > 0$ and $\sum_{i=1}^7 q_i = 1$. It can be verified that the first several moments of ζ_t are well approximated by the auxiliary representation. This means that we can modify (12) as follows:

$$\boldsymbol{\kappa} = \boldsymbol{I}_T \boldsymbol{h} + \boldsymbol{\epsilon}^\star, \quad \boldsymbol{\epsilon}^\star | \boldsymbol{q} \sim N(\boldsymbol{\nu}, \text{diag}(\boldsymbol{v})).$$

Given the conditional prior $\boldsymbol{h}|h_0, \sigma_h^2 \sim N(\mathbf{1}h_0, \sigma_h^2(\boldsymbol{H}'\boldsymbol{H})^{-1})$, we use the Bayesian regression lemma and derive the following conditional posterior:

$$\boldsymbol{h}|\boldsymbol{\eta}, h_0, \sigma_h^2, \boldsymbol{q} \sim N(\boldsymbol{\mu}_h, \boldsymbol{P}_h^{-1}),$$

where

$$\begin{aligned}
\boldsymbol{P}_h &= \frac{1}{\sigma_h^2}\boldsymbol{H}'\boldsymbol{H} + \text{diag}(-\boldsymbol{v}), \\
\boldsymbol{\mu}_h &= \boldsymbol{P}_h^{-1}\left(\frac{h_0}{\sigma_h^2}\boldsymbol{H}'\boldsymbol{e}_1 + \text{diag}(-\boldsymbol{v})(\boldsymbol{\kappa} - \boldsymbol{v})\right).
\end{aligned}$$

We then update the mixing components via a categorical distribution with the following conditional posterior:

$$P(q_t = i)|\kappa_t, h_t \propto \frac{q_i}{\sqrt{v_i}} \exp\left(-\frac{1}{2v_i}(\kappa_t - \nu_i - h_t)^2\right), \quad t = 1, ..., T.$$

1.3 Sample initializations

For $f \in \{h^S, h^F, h^C, \alpha, \beta, \lambda, \gamma, \delta\}$, we can write

$$\boldsymbol{H}\boldsymbol{f} = \mathbf{1}f_0 + \boldsymbol{\epsilon}^f, \quad \boldsymbol{\epsilon}^f|\sigma_f^2 \sim N(\mathbf{0}, \sigma_f^2\boldsymbol{I}_T).$$

Provided the diffuse prior shown in section 2.3 of the main text, or $f_0 \sim N(0, M)$ with $M = 10^6$, we have the conditional posterior given by

$$f_0|\boldsymbol{f}, \sigma_f^2 \sim N(\mu_{f_0}, \sigma_{f_0}^2),$$

where

$$\begin{aligned}
\frac{1}{\sigma_{f_0}^2} &= \frac{1}{M} + \frac{1}{\sigma_f^2}\boldsymbol{e}_1'\boldsymbol{e}_1, \\
\mu_{f_0} &= \frac{\sigma_{f_0}^2}{\sigma_f^2}\boldsymbol{e}_1'\boldsymbol{H}\boldsymbol{f}.
\end{aligned}$$

We can further simplify the expression above as follows:

$$f_0|f_1,\sigma_f^2 \sim N\left(\frac{f_1/\sigma_f^2}{1/M+1/\sigma_f^2},\left(\frac{1}{M}+\frac{1}{\sigma_f^2}\right)^{-1}\right).$$

A straightforward modification is made for the initialization of the common inflation trend, given by

$$\tau_0^C|\tau_1^C,\gamma_1,\delta_1,\epsilon_1^S,\epsilon_1^F,h_1^C \sim N\left(\frac{(\tau_1^C-\gamma_1\epsilon_1^S-\delta_1\epsilon_1^F)\exp(-h_1^C)}{1/M+\exp(-h_1^C)},\left(\frac{1}{M}+\exp(h_1^C)\right)^{-1}\right).$$

2 Mixing properties and posterior statistics of model parameters

All results obtained from the FCUC model presented in the main text, except for the expanding-window forecasting exercise, are based on a post-burn in sample of 10,000 MCMC runs (with 5,000 initial runs). We further thin the chain, so that the posterior sample of size $N = 2,500$ consists of every fourth draw obtained from the MCMC runs. Estimation takes approximately 6 minutes on a low-end laptop bought in 2015. Results based on 150,000 runs are virtually identical.

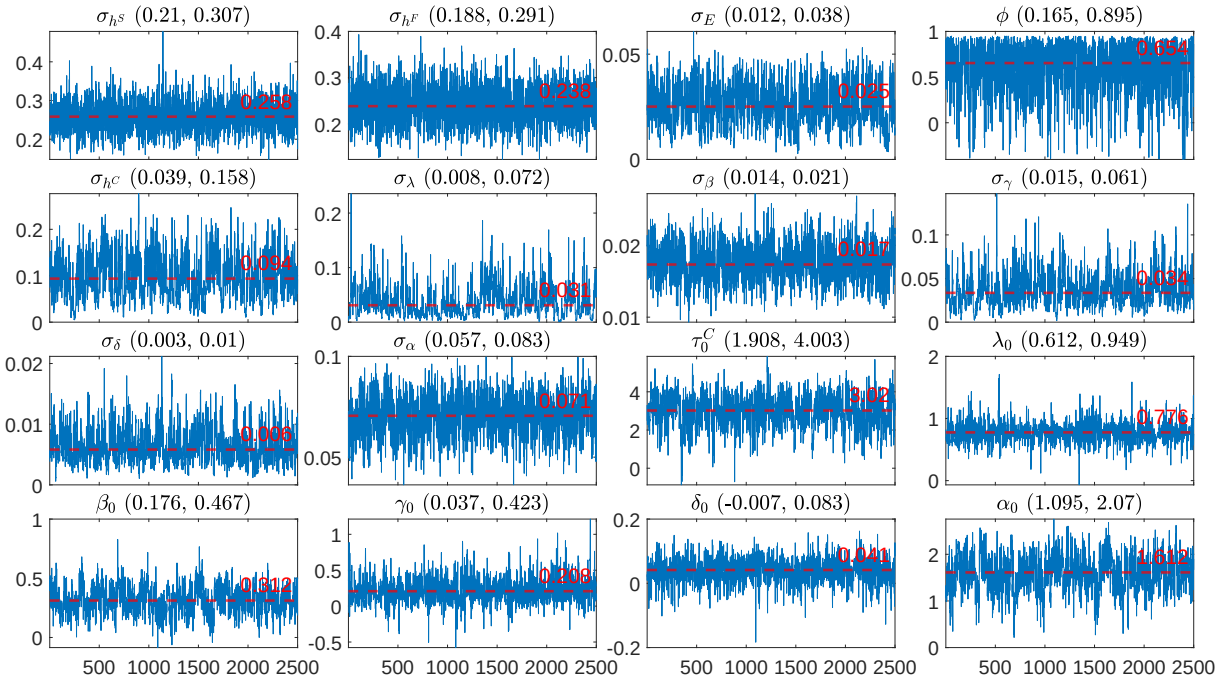

Figure 1: Posterior traces of parameters obtained from the FCUC model. Titles indicate parameters, following the same notations of the main text, and the 0.05 and 0.95 quantiles of their posterior distributions. Red lines and values show the posterior medians.

Figure 1 shows the posterior traces obtained from the post-burn in sample of the FCUC model parameters. We also indicate posterior quantiles, including the 5th, 50th, and 95th percentile of each parameter's posterior distribution. Visual inspection suggests satisfactory mixing of the Markov chain.

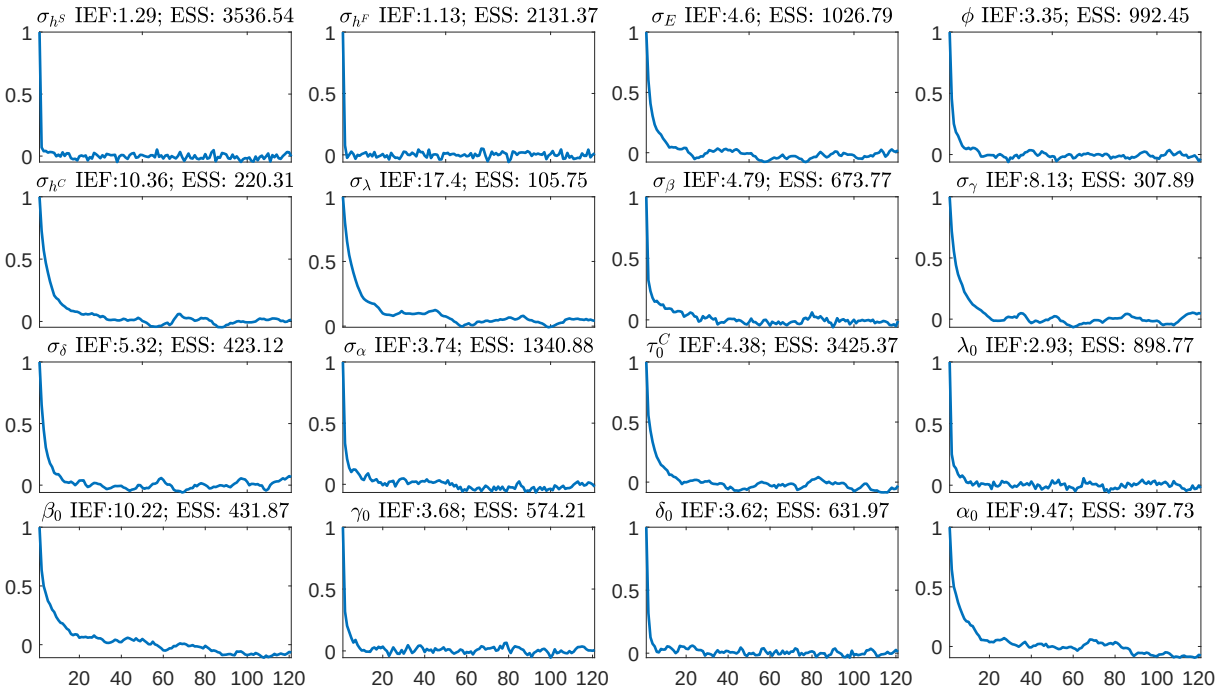

Figure 2: Autocorrelation functions of parameters obtained from the FCUC model. Titles indicate parameters, inefficiency factor (IEF) and effective sample size (ESS).

Figure 2 shows the autocorrelation function (ACF) of model parameters. For all plots, we observe that the ACFs converge to zero, which suggests a well-mixed Markov chain. The least efficient parameters are β_0 and α_0, the initialization parameters of the regression coefficients in the measurement equation of the long-run inflation expectations, *i.e.*, equation (4) in the main text. This may have to do with the fact that the majority of the information used for identifying trend inflation comes from the sticky and flexible inflation rate time series, with long-run inflation expectations offering only a marginal contribution. This result also resonates with our finding in the main text that long-run inflation expectations show persistent deviations from the assumption of rational expectations and their anchoring effect for the model is mainly effective during the two oil crises of the 1970s-80s.

We summarize the convergence diagnostics via the *inefficiency factor* (IEF) and the *effective sample size* (ESS), also reported in figure 2. The IEF measures the number of posterior draws

needed to achieve the same inferential accuracy as one independent draw from the posterior. Thus, we prefer smaller IEFs (closer to one). The ESS indicates the number of posterior draws that can be regarded as independent and, therefore, we prefer a larger ESS (closer to N, the posterior sample size). Following Robert et al. (1999), these are defined by

$$\begin{aligned}
\text{IEF}_n &= 1 + 2\sum_{i=1}^{n}\left(1 - \frac{i}{n}\right)\rho_i, \\
\text{ESS}_n &= \frac{N}{1 + 2\sum_{i=1}^{n}\rho_i},
\end{aligned}$$

where ρ_i denotes the i-th ACF of the posterior trace of a model parameter, $1-i/n$ is the sequence of Bartlett weights, and n is a chosen cutoff that truncates the ACF. We choose n to be 120. It matters little if we further increase the cutoff, as the Bartlett weights effectively end ρ_i at a linear rate, which is sufficient for a well-mixed chain. It can be shown that the IEF_n converges to the integrated autocorrelation time (long-run variance of the Markov chain, if scaled by the variance of the chain) as $n \to \infty$. If the chain is not convergent, then the IEF explodes.

A rule-of-thumb for valid posterior inference is that the ESS must be larger than $N/10$, which is satisfied by all the parameters of the FCUC model, even the least efficient ones, β_0 and α_0. For σ_{h^S}, the chain is highly well-mixed. Note that its ESS is larger than N. This, however, does not suggest a numerical issue, but simply shows the fact that we were too conservative and thinned the chain more than necessary. Therefore, the MCMC algorithm for the FCUC model behaves satisfactorily, yielding a well-mixed chain and enabling valid posterior inference.

References

Chan, J. C. and I. Jeliazkov (2009). Efficient simulation and integrated likelihood estimation in state space models. *International Journal of Mathematical Modelling and Numerical Optimisation 1*(1-2), 101–120.

Eisenstat, E., J. C. Chan, and R. W. Strachan (2016). Stochastic model specification search for time-varying parameter VARs. *Econometric Reviews 35*(8-10), 1638–1665.

Kim, S., N. Shephard, and S. Chib (1998). Stochastic volatility: likelihood inference and comparison with ARCH models. *Review of Economic Studies 65*(3), 361–393.

Robert, C. P., G. Casella, and G. Casella (1999). *Monte Carlo statistical methods*, Volume 2. Springer.